Comparative Medicine
Copyright 2022
by the American Association for Laboratory Animal Science

Vol 72, No 2
April 2022
Pages 63–77

Original Research

Th1/Th17-mediated Immunity and Protection from Peripheral Neuropathy in Wildtype and IL10$^{-/-}$ BALB/c Mice Infected with a Guillain–Barré Syndrome-associated *Campylobacter jejuni* Strain

Jean M Brudvig,[1-3] Matthew M Cluett,[1,3] Elizabeth U Gensterblum-Miller,[1,3] James Chen,[1,3] Julia A Bell,[1,3] and Linda S Mansfield[1-4,*]

***Campylobacter jejuni* is an important cause of bacterial gastroenteritis worldwide and is linked to Guillain–Barré syndrome (GBS), a debilitating postinfectious polyneuropathy. The immunopathogenesis of GBS involves the generation of antibodies that are cross reactive to *C. jejuni* lipooligosaccharide and structurally similar peripheral nerve gangliosides. Both the *C. jejuni* infecting strain and host factors contribute to GBS development. GBS pathogenesis is associated with Th2-mediated responses in patients. Moreover, induction of IgG1 antiganglioside antibodies in association with colonic Th2-mediated immune responses has been reported in *C. jejuni*-infected C57BL/6 IL10$^{-/-}$ mice at 4 to 6 wk after infection. We hypothesized that, due to their Th2 immunologic bias, BALB/c mice would develop autoantibodies and signs of peripheral neuropathy after infection with a GBS patient–derived strain of *C. jejuni* (strain 260.94). WT and IL10$^{-/-}$ BALB/c mice were orally inoculated with *C. jejuni* 260.94, phenotyped weekly for neurologic deficits, and euthanized after 5 wk. Immune responses were assessed as *C. jejuni*-specific and antiganglioside antibodies in plasma and cytokine production and histologic lesions in the proximal colon. Peripheral nerve lesions were assessed in dorsal root ganglia and their afferent nerve fibers by scoring immunohistochemically labeled macrophages through morphometry. *C. jejuni* 260.94 stably colonized both WT and IL10$^{-/-}$ mice and induced systemic Th1/Th17-mediated immune responses with significant increases in *C. jejuni*-specific IgG2a, IgG2b, and IgG3 plasma antibodies. However, *C. jejuni* 260.94 did not induce IgG1 antiganglioside antibodies, colitis, or neurologic deficits or peripheral nerve lesions in WT or IL10$^{-/-}$ mice. Both WT and IL10$^{-/-}$ BALB/c mice showed relative protection from development of Th2-mediated immunity and antiganglioside antibodies as compared with C57BL/6 IL10$^{-/-}$ mice. Therefore, BALB/c mice infected with *C. jejuni* 260.94 are not an effective disease model but provide the opportunity to study the role of immune mechanisms and host genetic background in the susceptibility to post infectious GBS.**

Abbreviations: GBS, Guillain–Barré syndrome; NOD, nonobese diabetic; OFT, open-field test; TSB, tryptic soy broth; TSAB, tryptic soy agar supplemented with 5% defibrinated sheep blood

DOI: 10.30802/AALAS-CM-21-000059

Campylobacter jejuni, a motile gram-negative bacterium, is a common cause of human bacterial gastroenteritis worldwide and is considered by the World Health Organization to be 1 of the 4 key global causes of diarrheal disease.[60] Although high numbers of *C. jejuni* can colonize chickens without causing apparent disease, infected people develop symptoms that typically include diarrhea, abdominal pain, and fever.[60,64] Although usually self-limiting, human campylobacteriosis has been linked to multiple postinfectious complications including irritable bowel syndrome, inflammatory bowel disease, reactive arthritis, and Guillain–Barré syndrome (GBS).[27,60] GBS is debilitating, with many patients experiencing protracted recovery and residual neurologic deficits.[57] This syndrome is clinically heterogeneous, but common characteristic symptoms include rapidly progressing limb weakness and reflex deficits. Pain, weakness, ataxia, and respiratory insufficiency are variably seen, depending on the specific GBS disease subtype present.[57] Estimates of GBS incidence after *C. jejuni* infection vary from 1 in 1000 to 5000 cases to 7 in 10,000.[27,57] Although several infectious agents have been associated with GBS, epidemiologic studies have identified *C. jejuni* as the most common antecedent infection in GBS;[20,26] one group estimated that among more than 2500 GBS cases, 31% were attributable to antecedent *Campylobacter* infection.[45]

Structural similarity between the lipooligosaccharides of some *C. jejuni* isolates and peripheral nerve gangliosides, such

Received: 08 Mar 2021. Revision requested: 07 May 2021. Accepted: 03 Sep 2021.
[1]Comparative Enteric Diseases Laboratory, Department of Large Animal Clinical Sciences; [2]Comparative Medicine and Integrative Biology; [3]College of Veterinary Medicine; and [4]Department of Microbiology and Molecular Genetics, Michigan State University, East Lansing, Michigan
Corresponding author. Email: mansfie4@cvm.msu.edu

as GM1, has been implicated in development of antiganglioside antibodies and GBS.[2,40,66] Antibodies to gangliosides, particularly to GM1 and often of the IgG isotype, are detected frequently in the sera of patients with GBS.[46] Furthermore, the presence of antiganglioside antibodies is correlated with slower patient clinical recovery and increased disability, and clinical improvement was seen with decreasing antiganglioside antibodies in patients with *C. jejuni*–associated GBS or the Miller–Fisher syndrome GBS subtype.[24,48] Ganglioside-like epitopes were found more frequently in lipooligosaccharides of *C. jejuni* isolates from patients with GBS or Miller–Fisher syndrome than in isolates from those with uncomplicated enteritis.[2] However, the presence of ganglioside-like moieties alone appears insufficient to elicit GBS, because the expression of ganglioside mimics can be found in *C. jejuni* isolates from enteritis patients without GBS.[2,54] These findings suggest a potential role for both *C. jejuni*–specific factors (for example, ganglioside mimics on the lipooligosaccharide) and host factors (for example, effects of the immunogenetic background on susceptibility to GBS after campylobacteriosis).

Murine models that resemble human *C. jejuni*-induced colitis[5,11,17,35,36] exploit features of the immune system, microbiota, or both to provide robust models that lack the transient or persistent asymptomatic colonization that have been observed in previous mouse models.[7,8] Of particular relevance to the current study was the development of a colitis model in IL10-deficient C57BL/6 mice after infection with *C. jejuni* 11168.[36] Development of age-related spontaneous enterocolitis in IL10$^{-/-}$ mice on different genetic backgrounds is well documented and results primarily from unchecked Th1-mediated immunologic responses to intestinal microbiota in the absence of the regulatory action of IL10.[6,29] This cytokine has important immunosuppressive effects, especially on monocytes and macrophages, and inhibits release of proinflammatory mediators.[50] In our previous studies, the absence of IL10 has proven critical for induction of inflammatory disease after *C. jejuni* infection in that WT mice infected with colitogenic *C. jejuni* strain 11168 are stably colonized but do not develop the severe colitis seen in infected IL10$^{-/-}$ mice.[9.36.37]

Robust animal models of human GBS have been difficult to develop. Models in species including mice,[21,51,62] rabbits,[65] and chickens[31,42] bear some similarity to various aspects of human disease. However, anatomic and physiologic differences between birds and humans limit the utility of the chicken model. Dogs will sometimes develop acute idiopathic polyradiculoneuritis that can serve as a model for the axonal form of human GBS but this canine condition is rare.[56] Furthermore, aside from the occurrence of spontaneous autoimmune peripheral polyneuropathy in mice,[51] the aforementioned mammalian models are experimentally induced, and disease induction requires injection of lipooligosaccharide,[65] myelin,[62] or antiganglioside antibody,[21] together with factors like Freund complete adjuvant[62,65] or normal human serum.[21]

Mouse models of GBS after oral infection with *C. jejuni* mimic the typical route of human infection.[9,35,55] C57BL/6 IL10$^{-/-}$ mice infected with *C. jejuni* 260.94, a strain isolated from a patient with GBS, developed Th2-mediated responses including the production of IgG1 antibodies to gangliosides GM1 and GD1a.[35] WT nonobese diabetic (NOD) mice and congenic IL10$^{-/-}$ and costimulatory molecule B7-2$^{-/-}$ mice infected with *C. jejuni* strain 260.94 showed greater generation of antiganglioside antibodies and macrophage and T-cell infiltration into peripheral nerves, including the sciatic nerve and dorsal root ganglia (DRG), as compared with controls.[55] The microbiota also contribute to antiganglioside antibody production after *C. jejuni* strain 260.94 infection in WT C57BL/6 mice; mice with a human-derived microbiota had higher anti-GM1 IgG1 antibodies than did mice with a conventional mouse microbiota.[9] These models showed that expression of ganglioside mimics in an infecting *C. jejuni* lipooligosaccharide elicited production of antiganglioside antibodies and was associated with peripheral nerve damage;[9,55] however, other factors may contribute.

The importance of host factors in determining susceptibility to GBS is poorly understood. Mouse strains with C57BL/6 and NOD backgrounds have been studied,[9,55] but the development of mouse models on additional genetic backgrounds could elucidate how the host immune response mediates GBS neuropathology. However, such studies must be performed rigorously using a similar study design for mouse strains anticipated to be informative. C57BL/6 IL10$^{-/-}$ mice infected with *C. jejuni* strain 11168 developed colitis and Th1/Th17-mediated immune responses, whereas mice of the same genotype infected with the GBS patient-derived *C. jejuni* strain 260.94 mounted Th2-mediated responses, including IgG1 that reacted with GM1 and GD1a gangliosides, but did not develop colitis.[35] Reports indicate that BALB/c and C57BL/6 mice have divergent immunologic response after infection with a number of pathogens.[32,33,39,58] In *Leishmania major* infections, BALB/c mice produce high amounts of IL4 and are susceptible to disease, whereas C57BL/6 mice downregulate IL4 production, produce IFNγ, and are relatively resistant to disease.[49] Multiple studies have demonstrated that upon in vitro stimulation, peritoneal macrophages, spleen cells, and dendritic cells derived from BALB/c mice exhibit a relative Th2 bias when exposed to various stimuli whereas C57BL/6 mice exhibit a more inflammatory, Th1-mediated bias.[32,33,39,58] In 2 studies of GBS patients, presence of type 2 IgG1 antiganglioside antibodies alone was associated with previous *C. jejuni* infection and worse clinical outcomes, whereas IgG3 antibodies, either alone or in combination with IgG1 antiganglioside antibodies, were associated with previous respiratory infection and better outcomes.[25,28] Therefore, we sought to develop a GBS model in mice that were characterized by Th2-biased responses after enteric infection and were likely to show strong IgG1 responses when inoculated orally with a patient-derived *C. jejuni* GBS strain.

We hypothesized that WT and IL10$^{-/-}$ BALB/c mice infected with *C. jejuni* 260.94 would 1) mount systemic and local gastrointestinal tract Th2-driven immune responses, including production of antiganglioside antibodies, without developing colitis and 2) develop gait abnormalities, neuromuscular weakness, and macrophage infiltration into peripheral nerves, reflecting *C. jejuni*-associated neuropathology. In addition, we hypothesized 3) that immune responses and neuropathology would be exacerbated in mice lacking antiinflammatory IL10. To test these hypotheses, BALB/c mice (WT and IL10$^{-/-}$) were orally infected with the *C. jejuni* GBS patient-derived strain 260.94, which expresses a GM1a ganglioside mimic.[34] This strain consistently colonized mice of NOD and C57BL/6 genetic backgrounds without inducing colitis[4,9,35,55] while producing antiganglioside antibodies[35,55] and nerve lesions.[55] We used ELISA to measure plasma anti-*C. jejuni*, anti-GM1, and anti-GD1a IgG antibody subtypes. A flow cytometry–based multiplex bead assay was used to measure cytokines in the proximal colon that reflected local Th-adaptive immune responses. Histologic lesions in the gastrointestinal tract were graded according to a previously published scale.[36] Neurologic phenotyping tests included DigiGait, open field test (OFT) and hang testing. Morphometry was used to quantify macrophages labeled immunohistochemically with F4/80 in lumbar DRG.

Results from this study indicate that *C. jejuni* 260.94 colonized BALB/c mice and induced a Th1/Th17 response that was exacerbated in IL10$^{-/-}$ mice but did not produce colitis. Significant differences in antiganglioside antibody isotypes were related to mouse genotype, but not to *C. jejuni* infection status, and did not correlate with increased macrophage numbers in DRG. No overt neurologic phenotype was observed in any experimental mouse. Thus, this reportedly Th2-biased mouse strain, when infected with a *C. jejuni* strain expressing ganglioside mimics in the outer core that was reported to induce a Th2 response in C57BL/6 IL10$^{-/-}$ mice, mounted predominantly Th1/Th17-mediated responses. The contrasting immune responses between mice of different genetic backgrounds after exposure to the same *C. jejuni* strain as reported in this study and previously[35] reinforce the role of host factors in determining susceptibility to GBS after *C. jejuni* infection. In addition, our results support the use of WT and IL10$^{-/-}$ mice on the BALB/c genetic background as an additional model for studying immune responses to *C. jejuni* infection.

Materials and Methods

Mice. All mouse experiments were performed according to recommendations in the *Guide for the Care and Use of Laboratory Animals* and NIH guidelines (04/07-044-00). All procedures were approved by the Michigan State University IACUC (approval numbers 06/12-107-00 and 06/15-101-00). BALB/cJ (referred to as BALB/c WT) and C.129P2(B6)-*Il10*^{tm1Cgn}/J (referred to as BALB/c IL10$^{-/-}$) mice were purchased from Jackson Laboratory (Bar Harbor, ME) and bred inhouse for a period of 2 y before use for these studies. Age-matched male and female mice used in the experiment were bred and maintained inhouse. Husbandry has been previously described.[36] The WT or IL10-deficient genotypes were verified by using a PCR assay offered by the Jackson Laboratory (https://www.jax.org/Protocol?stockNumber=014530&protocolID=28729). DNA extracted from feces or cecal tissue collected from experimental mice used in this study was screened for enteric pathogens including *Citrobacter rodentium*, *Enterococcus faecium* and *E. faecalis*, *Helicobacter* spp., and *Campylobacter* spp. by PCR analysis as previously described.[36] Sentinel mice housed in the same rack as experimental mice were tested for *Corynebacterium bovis*, pinworms, and fur mites and by serologic evaluation for antibodies to epidemic diarrhea of infant mice virus, mouse hepatitis virus, mouse parvovirus, minute virus of mice (parvovirus type), and Theiler murine encephalomyelitis virus. These mice were also tested by PCR assay for *Aspiculuris tetraptera*, *Corynebacterium bovis*, *Myocoptes*, *Radfordia/Myobia*, *Syphacia muris*, and *Syphacia obvelata.* Finally, pelt swabs from these mice were tested for *Corynebacterium bovis, Myocoptes*, and *Radfordia/Myobia*. All test results were negative. Prior to inoculation, mice were transported to the Michigan State University Research Containment Facility. The mice were housed individually after a 1-wk acclimation. At humane gastrointestinal and neurological disease endpoints that we described earlier[36,55] or at the end of the experiment, all mice were euthanized by CO_2 overdose according to AVMA guidelines (https://www.avma.org/KB/Policies/Pages/Euthanasia-Guidelines.aspx).

Experimental design. Prior to this study, the ability of *C. jejuni* 260.94 to colonize BALB/c WT mice was verified by inoculation of 5 mice with *C. jejuni* 260.94 (dose, 3.7×10^9 cfu) by gastric gavage; 3 mice inoculated with tryptic soy broth (TSB; sham/vehicle) served as controls. The inoculum was prepared and the confirmation of *C. jejuni* 260.94 colonization by culture and PCR analysis for this pilot study were performed as described in the following section.

The primary study used 40 mice (20 BALB/c WT and 20 BALB/c IL10$^{-/-}$ mice). Mice of each genotype were randomized with regard to sex, litter, treatment group, and cage position on the rack. Mice were inoculated at 14 to 15 wk of age. Specifically, 10 BALB/c WT and 10 BALB/c IL10$^{-/-}$ mice received TSB; likewise, 10 BALB/c WT and 10 BALB/c IL10$^{-/-}$ mice received *C. jejuni* 260.94. BALB/c WT mice were inoculated 1 wk before BALB/c IL10$^{-/-}$ mice. Both groups were euthanized 5 wk after their respective inoculation.

Preparation and inoculation of *C. jejuni* inoculum. *C. jejuni* strain 260.94 originally obtained from American Type Culture Collection (strain BAA-1234; Vienna, VA) and stored as glycerol stock cultures at –80 °C was used in this study. The inocula for the BALB/c WT and BALB/c IL10$^{-/-}$ groups were prepared as previously described.[36] Briefly, for each preparation, inoculum from frozen stock was streaked onto tryptic soy agar plates supplemented with 5% defibrinated sheep blood (TSAB plates; Cleveland Scientific, Bath, OH). The plates were incubated for approximately 24 h at 37 °C in vented anaerobic jars. Generation of the microaerobic environment was achieved by evacuation to –25 cm Hg followed by equilibration with a gas mixture comprising 80% N_2, 10% CO_2, and 10% H_2. Colonies were harvested, suspended in TSB, spread into lawns on fresh TSAB plates, and incubated overnight at 37 °C in the microaerobic environment. The following day, lawns were harvested and suspended in TSB, aiming to achieve an optical density at 600 nm of approximately 1.0 in a 1:10 dilution of culture. Motility, spiral morphology, and purity of both inoculums were confirmed by wet mount and Gram stain preparations. Mice were inoculated with 0.1 mL of *C. jejuni* 260.94 or TSB via intragastric gavage by using a 3.5-French red rubber catheter. Immediately before and after inoculation, the inocula were serially diluted in TSB and spread on TSAB plates, and the plates incubated at 37 °C in the microaerobic environment for approximately 48 h. Final calculated doses of *C. jejuni* 260.94 inocula were 3.1×10^8 cfu for BALB/c WT mice and 2.8×10^8 cfu for BALB/c IL10$^{-/-}$ mice.

Monitoring for clinical signs. Starting at inoculation, mice were checked at least once daily for clinical signs. Evaluated clinical parameters included observation of eating and drinking and overall activity level and gauging abnormalities in respiratory rate, hair coat, posture (for example, hunching), defecation including diarrhea, and level of movement including rearing. Any mouse reaching a predetermined gastrointestinal or neurological humane endpoint[36,55] was immediately euthanized, and necropsy was performed. Early euthanasia was required for only one mouse, as described in the results section.

Neurologic phenotyping. Mice underwent phenotyping tests weekly to evaluate clinical signs of neurologic disease, including gait abnormalities and loss of motor strength. Assessments included treadmill analysis, hang test, and OFT. Before inoculation, mice were acclimated to these tests for 1 wk before the start of the experiment. Baseline data collected prior to inoculation were included in the statistical analyses.

Treadmill imaging system. The DigiGait (Mouse Specifics, Quincy, MA) treadmill system records numerous gait indices to allow detection of subtle gait abnormalities. Each mouse was placed on a transparent moving belt. A digital camera underneath the belt captured movement using DigiGait Video Imaging Acquisition software (Mouse Specifics). Data were recorded over a 3-s run in which the mouse ran in the center of the belt, with no or minimal leaning against the clear plastic siding or contact with the front or back bumpers. Digital images were then processed by using the DigiGait Imaging Analysis software (Mouse Specifics). Numerical data reflecting multiple

gait parameters are calculated for each limb and exported to an Excel spreadsheet for statistical analysis. Of the 42 available gait parameters, 8 were deemed most relevant for analysis:[14,22,44] swing (in seconds), propel (seconds), stance (seconds), stride (seconds), stride length (centimeters), stride frequency (steps per second), absolute paw angle (degrees), and stance width (centimeters). In this study, the mice were recorded running at speeds of 25 cm/s, 30 cm/s, and 35 cm/s. When needed, mice were given multiple chances to achieve a 3-second run, with rest periods between attempts. The belt was cleaned with 70% ethanol between mice.

Hang test. The hang test served as a measure of motor strength and balance. This test was performed as described[12,55] with minor modifications. Briefly, each mouse was placed on a square metal grid elevated several inches above its cage and allowed to grip the metal. A stopwatch was started when the grid was flipped upside down. Mice were allowed to hang for a maximum 60 s, and the time elapsed until they fell from the grid into the cage was recorded. This process was performed a total of 3 times, with a 60 s rest between trials. The grid was cleaned with 70% ethanol between mice. The average time to fall (or a maximum of 60 s when the mouse did not fall) over the 3 trials was used in the analyses.

OFT. The OFT allows assessment of gait, posture, and activity level. The OFT was performed by allowing the mouse to move freely within a clear plastic standard 18 in. × 8 in. rat cage with 4 quadrants demarcated on the bottom. The activity of the mouse was recorded for 60 s, beginning with its placement in the center of the cage, by using a stationary video camera mounted on a tripod and set at approximately the same angle each week. At the end of each video, the mouse number was shown, with genotype and treatment group de-identified to eliminate bias. The cage was cleaned with 70% ethanol between mice. Parameters intended for assessment included the number of quadrants crossed, number of rears, and gait or posture abnormalities such as increased stance width or splayed toes.

Necropsy procedures. Mice were euthanized by CO_2 overdose at 5 wk after inoculation. Immediately thereafter, mice were weighed, and blood samples were collected via cardiocentesis using a 1-mL tuberculin syringe loaded with 0.1 mL 3.8% sodium citrate.

Instruments tips were sterilized between manipulations sections of the gastrointestinal tract by placing them in a hot bead sterilizer for 2 min. The cecum was excised including approximately 0.5 to 1 cm of adjoining proximal colon and ileum. The tip of the cecum was removed for bacteriology studies. The remaining ileocecocolic junction was infused with 10% neutral phosphate-buffered formalin (Fisher Scientific, Hampton, NH), placed on a sponge in a histologic tissue cassette (Fisherbrand Histosette II Tissue Cassette, Fisher HealthCare, Pittsburgh, PA), and immersed in 10% neutral phosphate-buffered formalin.

Sections of stomach, jejunum, and proximal colon and the tip of the cecum were excised and rinsed in PBS. Each tissue specimen was divided into 3 sections: 2 were snap-frozen in microfuge tubes and cryovials, and the third was streaked onto *Campylobacter*-selective medium[36] (i.e., TSAB plates containing cefoperazone [20 µg/mL], vancomycin [10 µg/mL], and amphotericin B [2 µg/mL]); antimicrobials were obtained from Sigma–Aldrich (St Louis, MO). Plates were placed into air-tight jars with a Campy*Gen* sachet (Oxoid, Basingstoke, Hampshire, United Kingdom). Fecal pellets were collected into microfuge tubes and placed on ice.

DRG and their afferent nerve fibers were collected from experimental mice for histologic and morphologic analysis in a 2-step procedure. At the time of necropsy, each mouse was skinned and the muscles overlying the spine were removed. The roof of the vertebral canal was removed using Castroviejo microsurgical scissors to expose the spinal cord. Muscle and connective tissue were bluntly dissected to expose the sciatic nerve on each side. Thereafter, the carcass was submerged in 10% neutral buffered formalin in a specimen cup for dissection of tissues at a later date.

Snap-frozen tissues were stored at –80 °C. Gastrointestinal samples streaked on *Campylobacter*-selective plates in the air-tight jars were placed at 37 °C. Fecal pellets in TSB containing 15% glycerol were mashed by using a sterile applicator stick, vortexed, spread onto *Campylobacter*-selective plates, and incubated at 37 °C in jars with the microaerobic environment generated by evacuation and equilibration with the gas mixture. Plasma was separated from whole blood by centrifugation, harvested, and stored at –80 °C until analysis. The cassettes containing ileocecocolic samples and the carcasses for nerve dissection were transferred from formalin to 60% ethanol after 24 and 48 h, respectively.

Confirmation of colonization via culture and PCR analysis. Colonization of stomach, jejunum, cecum, colon, and feces was reported according to a semiquantitative grading system of plate coverage by *C. jejuni* colonies[36] after 48 to 72 h of incubation: 0, no growth; 1, light growth (approximately 1 to 20 cfu); 2, moderate growth (20 to 200 cfu); 3, heavy growth (more than 200 cfu); and 4, confluent growth.

To confirm that infected mice were colonized by *C. jejuni* 260.94 and to exclude colonization in sham-inoculated mice, *C. jejuni*-specific PCR analysis for the *C. jejuni gyrA* gene was conducted at necropsy.[36,61] For culture-positive mice, isolates of *C. jejuni* from cecal samples obtained at necropsy were used. For culture-negative infected mice and sham-inoculated mice, DNA was extracted from frozen cecal tissues obtained at necropsy by using a commercial kit (DNEasy Blood and Tissue Kit, Qiagen, Valencia, CA).

Pathologic changes: gastrointestinal tract. Gross lesions in the gastrointestinal tract and changes in the ileocecocolic lymph node and spleen noted during necropsy were recorded as noted by a veterinarian (JMB) and other experienced personnel. The ileocecocolic samples were processed routinely by the Investigative Histopathology Laboratory (Division of Human Pathology, Michigan State University). Briefly, tissue samples were embedded in paraffin, sectioned at 4 to 5 µm, stained with hematoxylin and eosin, and coverslipped. The ileocecocolic preparations were examined histologically by a board-certified veterinary clinical pathologist (JMB) who was blind to genotype and treatment groups. Lesions were graded by using a previously published scoring system.[36] The scale encompasses changes in the lumen (exudates, excessive mucus), epithelium (surface integrity, goblet cell hypertrophy or depletion, crypt abnormalities), lamina propria (inflammatory cell infiltrates), and submucosa (inflammation, edema, fibrosis). Raw scores (maximum, 42) were ranked as semiquantitative grades: 0 (0 to 9 points; no colitis), 1 (10 to 19 points; mild colitis), or 2 (20 or more; moderate or severe colitis).

ELISA. Plasma was stored in aliquots to prevent repeated freeze–thaw cycles. Anti-*C. jejuni* and antiganglioside GM1 and GD1a antibody isotypes including IgG1, IgG2a, IgG2b, and IgG3 were evaluated. The assays were performed as previously described.[17,36] Briefly, 96-well plates (Nunc Maxisorp, Thermo Scientific, Rochester, NY) were coated with antigen and incubated at 4 °C overnight. Antigens were diluted in PBS to the following concentrations: *C. jejuni* antigen,[36] 1.9 µg/mL;

GM1 antigen (US Biologic, Swampscott, MA), 2 µg/mL; GD1a antigen (Sigma–Aldrich, St. Louis, MO) 20 µg/mL. The plates were blocked with blocking buffer (10 mM PBS containing 3% BSA and 0.05% Tween20 [Sigma]) overnight at 4 °C. After 3 washes in wash buffer (PBS with 0.025% Tween20), plasma samples diluted in blocking buffer (all samples were diluted 1:25, except for anti-*C. jejuni* IgG2b and IgG2a, which were diluted at 1:100) were loaded in triplicate. Positive controls included plasma from mice from previous experiments with a high optical density or commercially available antibodies (anti-GD1a IgG1, EMD Millipore, Temecula, CA). Negative controls included anti*Toxoplasma gondii* antibody (ViroStat, Portland, ME) and wells including only blocking buffer. Sealed anti-GM1 and anti-GD1a antibody plates were incubated with samples overnight at 4 °C, whereas anti-*C. jejuni* antibody plates were incubated for 1 h on a platform shaker. Plates were washed, and secondary antibodies (Biotin-SP–conjugated AffiniPure Goat AntiMouse IgG1, IgG2a, IgG2b, IgG2c, or IgG3; Jackson ImmunoResearch, West Grove, PA) diluted in blocking buffer were added. After incubation for 1 h on a platform shaker, plates were washed again and ExtrAvidin peroxidase (Sigma–Aldrich; diluted 1:2000 in 10 mM PBS containing 1% BSA and 0.05% Tween20) was added. Plates were incubated for 1 h on a platform shaker and washed, and tetramethylbenzidine (TMB substrate; Rockland Immunochemicals, Gilbertsville, PA) was added. The reaction was stopped by adding 2 N H_2SO_4. Absorbance was read at 450 nm by using a model EL800 Universal Microplate Reader with KC Junior software (Bio-Tek Instruments, Winooski, VT). In a few samples, the coefficient of variance for triplicate values was 10% or greater. In these cases, if a clear outlier was present, that value was excluded. The absorbance generated from the diluent (blocking buffer) alone was subtracted from the mean absorbance obtained for each sample run in triplicate. This adjusted value was used in statistical analyses. Negative values generated by subtracting the absorbance of the blocking buffer from the mean sample absorbance were treated as 0 for the purpose of statistical analysis.

Measurement of colonic cytokine production. Rinsed samples of proximal colon collected in microfuge tubes and snap-frozen at necropsy were stored at –80 °C until analysis. Samples were thawed on ice and wet weight was recorded. Samples were homogenized on ice for 1 min in 400 µL of Hanks Balanced Salt Solution (Sigma) containing 0.5% Triton X100 (Sigma) and protease inhibitors (Roche cOmplete Mini EDTA-free Protease Inhibitor cocktail, Sigma) by using a microtube pellet pestle rod powered by a handheld Kontes pellet pestle motor. Homogenates were centrifuged at 12,000 × *g* for 30 min at 4 °C, and supernatants were aliquoted into cryovials and stored at –80 °C until analysis.

Cytokines were measured by using a flow cytometry–based multiplex bead assay panel (LEGENDPlex Mouse Th Cytokine Panel, BioLegend, San Diego, CA). Cytokines included in the panel are designed to characterize the adaptive immune response by delineating Th polarization. Analytes included IFNγ, TNFα, IL2, IL4, IL5, IL6, IL9, IL10, IL13, IL17A, IL17F, IL21, and IL22. Prior to analysis, aliquoted supernatants of the colon homogenates were thawed on ice and centrifuged at 300 × *g* for 10 min at 4 °C. The assay was performed by using undiluted supernatant and a V-bottom microplate according to the manufacturer's instructions. Data were acquired on a FACSCanto II flow cytometer (BD Biosciences, San Jose, CA) and analyzed by using LEGENDplex Data Analysis software (BioLegend). A standard curve was generated for each analyte. Each cytokine had a maximum standard concentration of 10,000 pg/mL. Data are presented as the number of picograms per milligram of tissue weight.

Assessment of nerve histopathology. Dissection of fixed tissue was performed using a dissecting microscope and nerves and dorsal root ganglia were embedded en bloc in a single cassette. Two or 3 lumbar DRG were harvested from the left side of the mouse. Where possible and in many cases, connections from the sciatic nerve to one or all DRG collected, including those in L3, L4, or L5 regions, were visualized prior to removal of DRG. The left sciatic nerve, brachial plexus, and lumbar DRG were placed in a cassette and stored in 60% ethanol until submission for histopathology.

The Investigative Histopathology Laboratory (Division of Human Pathology, Michigan State University) labeled sections immunohistochemically for the mouse macrophage marker F4/80. Specimens were embedded in paraffin and sectioned on a rotary microtome at 4 µm. Sections were placed on charged slides and dried at 56 °C overnight, deparaffinized in xylene, and hydrated through descending grades of ethyl alcohol to distilled water. Slides were then placed in Tris-buffered saline (pH 7.4; Scytek Labs, Logan, UT) for 5 min for pH adjustment. Epitope retrieval was performed by using Citrate Plus Retrieval Solution (pH 6.0; Scytek) in a vegetable steamer for 30 min followed by a 10-min countertop incubation with several changes of distilled water. After pretreatment, standard avidin–biotin complex staining steps were performed at room temperature on an autostainer (Dako, Agilent, Santa Clara, CA). All staining steps were followed by 2-min rinses in Tris-buffered saline containing Tween20 (Scytek Labs). After blocking nonspecific proteins by incubating in normal rabbit serum (Vector Labs, Burlingame, CA) for 30 min, sections were incubated with avidin (avidin D, Vector Labs) and biotin (D-biotin, Sigma) for 15 min each. Primary antibody slides were incubated for 60 min with monoclonal rat antimouse F4/80 (dilution, 1:100; AbD, Serote, Raleigh, NC) in Normal Antibody Diluent (Scytek Labs), then incubated for 30 min biotinylated rabbit antirat IgG (H + L mouse absorbed; prepared at 10.0 µg/mL in Normal Antibody Diluent), followed by incubation for 30 min in R.T.U. Vector Elite Peroxidase Reagent (Vector Labs). Reaction development used incubation for 15 in Nova Red Kit peroxidase chromogen (Vector Labs) followed by counterstaining in Gill 2 Hematoxylin (Cancer Diagnostics, Durham, NC) for 30 s, differentiation, and dehydration, clearing, and mounting (Permount, Fisher Scientific).

The number of F4/80-positive cells was quantified morphometrically. Images were analyzed by using ImageJ software (version 2.0.0rc-49/1.51d; distributed by Fiji [Fiji Is Just ImageJ]) for Windows (http://imagej.net/Fiji/Downloads).[52,53] The investigator (MMC) was blind to mouse genotype and treatment group. Contiguous images of each DRG section obtained at a magnification of 100× (10× objective) were opened in the ImageJ program. Positive cells were marked on the image by using the Cell Counter plugin. After all positive cells were marked, the area was outlined by using the Freehand Selections Tool. When necessary, multiple areas were traced individually, and the sum of the areas was recorded. Results are given as the number of F4/80-positive cells per area, with area representing 100,000 pixels. Finally, the slides were unblinded for statistical analysis.

Statistical analyses. Analyses were performed by using commercially available statistical software packages (GraphPad Prism version 6.00 for Windows, GraphPad Software, La Jolla, CA; SigmaStat 3.5 for Windows, Systat Software, Point Richmond, CA) and online statistical applications (VassarStats Website for Statistical Computation; vassarstats.net). Descrip-

tive data are expressed as mean ± SEM. P values of <0.05 were considered to be statistically significant.

DigiGait data generated for individual limbs were analyzed by using 2-way repeated-measures ANOVA followed by the Holm–Sidak multiple-comparisons test. These analyses were conducted by using SigmaStat because of missing values for weeks in which a mouse was unwilling to run on the DigiGait; SigmaStat uses a general linear model to generate a best estimate of the missing values. The mice were first grouped according to combined genotype and treatment group (for example, [WT TSB], [IL10$^{-/-}$ *C. jejuni* 260.94]) to compare all experimental mice together. Subsequent analyses evaluated differences in all parameters between control and infected groups for WT mice alone and for IL10$^{-/-}$ mice alone. Data were tested for normality and equal variance. Data that did not meet the assumption of equal variance were not analyzed. This applied only to a few specific DigiGait outcome measures (e.g., swing of a paw). Data from the hang test were analyzed by using 2-way repeated-measures ANOVA followed by the Holm–Sidak multiple-comparisons test.

The Freeman–Halton extension of the Fisher Exact Probability test was used to assess differences in colonization identified by culture between infected BALB/c WT and infected BALB/c IL10$^{-/-}$ mice. For this analysis, semiquantitative colonization grades included 0 (0 cfu), 1 (1 to 20 cfu), 2 (20 to 200 cfu), and 3 (more than 200 cfu, including grades of more than 200 cfu and confluent growth).

Gross pathology in sham-inoculated and *C. jejuni* 260.94-infected BALB/c IL10$^{-/-}$ mice was assessed similarly by using the Freeman–Halton extension of the Fisher Exact Probability test. For this analysis, gross pathology changes recorded at necropsy, including enlarged or thickened proximal colon, enlarged cecum, enlarged spleen, and enlarged ileocecocolic lymph node, were graded as 0 (no changes), 1 (1 change), or 2 (2 changes).

Due to the lack of independence of observations comprising the composite score, ranks of colitis scores were analyzed by using the Freeman–Halton extension of Fisher Exact Probability test performed on overall group data, followed by 6 pairwise comparisons. In addition, Kruskal–Wallis one-way ANOVA on ranks, followed by the Dunn posttest, was performed on raw histopathology scores.

Data obtained from plasma ELISA, colon cytokine measurements, and F4/80 scoring of DRG and afferent nerve fibers were analyzed by using nonparametric Kruskal–Wallis one-way ANOVA, which was followed by the Dunn multiple-comparisons test when overall significance was found.

Results

Confirmation of mouse genotype and absence of enteropathogens. Genotype (WT or IL10$^{-/-}$) was confirmed by PCR analysis of DNA obtained from cecal tissue of all mice. All mice were confirmed to be PCR-negative for all enteropathogens tested (*Citrobacter rodentium*, *Enterococcus faecium* and *E. faecalis*, *Helicobacter* spp., and *Campylobacter* spp.).

Clinical signs. One infected BALB/c WT mouse required early euthanasia at 14 d after infection due to a progressively worsening hunched posture, mildly decreased activity, roughened coat, thin body condition, and mildly increased respiratory effort. Necropsy revealed a large thoracic mass, which was considered to be unrelated to *C. jejuni* infection and was not further investigated. Due to morbidity unrelated to *C. jejuni* infection and the time span between the euthanasia of this mouse and the remaining experimental mice (approximately 3 wk), data for this mouse are included in the results of colonization but other experimental parameters are not. Questionable or mildly hunched posture, decreased activity, and hair coat quality were monitored carefully and were noted at least once during the study in 3 of the 10 sham-inoculated WT mice, 7 of the 10 infected WT mice, 5 of the 10 sham-inoculated IL10$^{-/-}$ mice, and 6 of the 10 infected IL10$^{-/-}$ mice. Many of these signs were attributed to characteristic BALB/c posture or hair coat appearance. No other mice required early euthanasia, and the remaining 39 experimental mice were euthanized at 5 wk after inoculation.

Neurologic phenotyping. Of all neurologic phenotyping tests, the results of the DigiGait treadmill analysis were most informative. Data from the OFT were not analyzed because the mice did not display enough spontaneous activity to provide sufficient information regarding rearing, quadrant crossing, or gait abnormalities.

Treadmill analysis system. Images recorded at 25 cm/s were processed because the most mice consistently ran at this speed each week. An infected male BALB/c IL10$^{-/-}$ mouse with several weeks of missing data was excluded from analysis. A few metrics failed equal variance and were excluded from results: right hindlimb stride and stride length in the combined analysis; left hindlimb swing in the IL10$^{-/-}$-only analysis; and left forelimb absolute paw angle in the WT-only analysis. We have reported only the data having a P value of less than 0.05 for either treatment group or time in the overall analysis (Table 1). Significant differences related to week of testing were found for multiple parameters, most frequently involving baseline and week 4. Significant treatment-group differences were identified for the forelimbs, including stance width and paw angle. When WT and IL10$^{-/-}$ genotypes were analyzed together (combined analysis), infected IL10$^{-/-}$ mice had a wider forelimb stance width than sham-inoculated WT mice. When the genotypes were analyzed separately, forelimb stance width was wider in infected than in sham-inoculated WT mice, but the difference was not significant for IL10$^{-/-}$ mice. In addition, the combined analysis showed a significant effect of treatment group for absolute paw angle of the right forelimb, but no pairwise comparisons were significant. Collectively, these data suggest that a relatively small proportion of gait parameters analyzed were affected by *C. jejuni* infection.

Hang test. No significant differences were found between treatment groups ($P = 0.199$). However, time had a significant effect ($P < 0.001$) emerged, with significant differences in pairwise comparisons between baseline and weeks 2, 4, and 5 (data not shown).

Colonization. At euthanasia, 9 of the 10 infected mice from each group were culture-positive in at least one area of the gastrointestinal tract. Although samples from the gastrointestinal tract included stomach, jejunum, cecum, colon, and feces, the cecum has been reported to be the most consistently and heavily colonized area of the gastrointestinal tract;[36,37] therefore results from the cecum are shown (Figure 1). Culture results positive for *C. jejuni* 260.94 among all samples from infected WT BALB/c mice ($n = 10$) were as follows: stomach, 1; jejunum, 7; cecum, 8; proximal colon, 9; and feces, 9. Culture results positive for *C. jejuni* 260.94 among infected BALB/c IL10$^{-/-}$ mice ($n = 10$) were: stomach, 1; jejunum, 0; cecum, 9; proximal colon, 9; and feces, 8. PCR analysis for the *C. jejuni gyrA* gene was positive for all isolates cultured from necropsy samples. All 20 TSB-inoculated mice were negative for *C. jejuni* by culture in all 5 areas sampled from the gastrointestinal tract. The 2 infected but culture-negative mice and all sham-inoculated mice were negative for *C. jejuni* by *gyrA* PCR on DNA isolated from frozen cecal tissue. Results of the Fisher Exact Probability test showed

Table 1. Results of DigiGait analysis

Gait parameter	*P*	Significant comparison
Analysis including both genotypes		
LH propel	0.011	Week: baseline compared with week 4
LH stance	0.049	Week: pairwise comparisons nonsignificant
RH propel	<0.001	Week: baseline compared with weeks 2, 3, 4, and 5 and weeks 1 compared with 3
RH stance	0.017	Week: baseline compared with week 4
RH absolute paw angle	0.042	Week: pairwise comparisons nonsignificant
LF absolute paw angle	0.017	Week: baseline compared with week 4
LF stance width	0.003	Treatment group: IL10$^{-/-}$ 260.94 compared with WT TSB
RF absolute paw angle	0.031	Treatment group: pairwise comparisons nonsignificant
RF absolute paw angle	0.010	Week: baseline compared with weeks 4 and 5
Analysis within BALB/c WT mice		
RH absolute paw angle	0.031	Week: week 1 compared with 3
LF stance width	0.034	Treatment group: 260.94 compared with TSB
Analysis within BALB/c IL10$^{-/-}$ mice		
LH propel	0.017	Week: baseline compared with weeks 2 and 4
LH stance	0.035	Week: baseline compared with week 4
RH propel	<0.001	Week: baseline compared with weeks 3, 4, and 5
LF absolute paw angle	0.021	Week: baseline compared with week 4
RF absolute paw angle	0.004	Week: baseline compared with weeks 3, 4 and 5

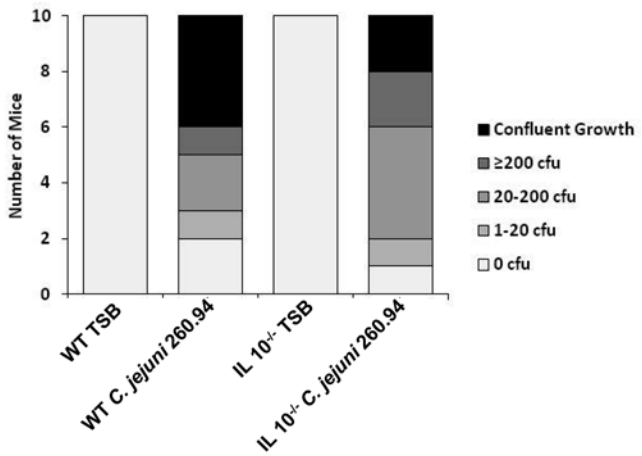

Figure 1. Culture results of *Campylobacter jejuni* 260.94 colonization of the cecum at the time of necropsy. WT and IL10-knockout (IL10$^{-/-}$) BALB/c mice were inoculated with either *C. jejuni* 260.94 or vehicle (tryptic soy broth, TSB). Colonization rates were semiquantitatively graded according to approximate number of colony-forming units on the plate. Except for one infected WT mouse requiring early euthanasia unrelated to *C. jejuni* infection, mice were euthanized at 5 wk after infection. Colonization in the cecum was not significantly different between infected WT and IL10$^{-/-}$ mice (Fisher Exact Probability test, $P_B = 0.775$).

no significant difference in colonization of the cecum between infected BALB/c WT and IL10$^{-/-}$ mice ($P_B = 0.775$).

Gross pathology and histologic assessment of colitis. Gross pathologic changes seen at necropsy included enlarged or thickened proximal colon, enlarged cecum, enlarged spleen, and enlarged ileocecocolic lymph node. Gross pathology in WT mice was minimal, regardless of infection status. Nearly all mice exhibiting one or more gross pathologic changes were BALB/c IL10$^{-/-}$ mice, regardless of *C. jejuni* 260.94 infection status (Figure 2 A). Of the 10 sham-inoculated IL10$^{-/-}$ mice, 9 had an enlarged or thickened proximal colon, and one also had an enlarged spleen. Similarly, 8 of the 10 *C. jejuni*-infected IL10$^{-/-}$ mice had an enlarged or thickened proximal colon; of these 8 mice, 3 also had an enlarged spleen, one also had an enlarged lymph node, and one also had a thickened cecal wall. Because only one mouse from each of the WT treatment groups had only one gross pathologic change and the remaining mice from both groups had no changes, gross pathology was not further analyzed in WT mice. Within BALB/c IL10$^{-/-}$ mice, comparison of gross pathology between sham-inoculated and *C. jejuni* 260.94-infected mice was assessed by using the Fisher Exact Probability test. No significant difference was found in gross pathology between infected and control IL10$^{-/-}$ mice ($P_B = 0.087$).

Histologic scoring of the ileocecocolic area placed all mice from all 4 treatment groups into grade 0 (0 to 9 points; no colitis) or grade 1 (10 to 19 points; mild colitis). As with changes noted grossly, more BALB/c IL10$^{-/-}$ mice than BALB/c WT mice had histologic lesions in the ileocecocolic junction, regardless of *C. jejuni* infection status (Figure 2 B). All 10 sham-inoculated and all 9 *C. jejuni*-infected WT mice had scores of less than 10, indicating no colitis. The TSB-inoculated IL10$^{-/-}$ mice showed the greatest range of raw scores (3 to 17 points) of any of the 4 treatment groups. Of the 10 sham-inoculated IL10$^{-/-}$ mice, 4 had mild colitis (score, 10 to 17); the remaining 6 mice in this group had no colitis (score, ≤ 9). The most frequent changes seen in TSB-inoculated IL10$^{-/-}$ mice were subjectively mild, reflecting the numerical score in the mild colitis category, and included luminal exudates comprising mucus and few neutrophils, damage to single cells in the surface epithelium, goblet cell depletion, crypt hyperplasia, increased mononuclear cells in the lamina propria, and extension of inflammation into the submucosa. Similarly, 4 of the 10 *C. jejuni*-infected IL10$^{-/-}$ mice had mild colitis (score, 11 to 16), whereas the remaining 6 mice in this group had no colitis (score, ≤ 9). Pathologic changes seen in *C. jejuni*-infected IL10$^{-/-}$ mice with mild colitis were similar to those seen in sham-inoculated mice and included mucus and a few neutrophils in the lumen, damage to single cells in the surface epithelium, goblet cell depletion, crypt hyperplasia, increased mononuclear cells in the lamina propria, and extension of inflammation into the submucosa (2 of 4 mice). Although significant differences were seen overall by using both the Fisher Exact Probability test on ranked data ($P_B = 0.012$) and

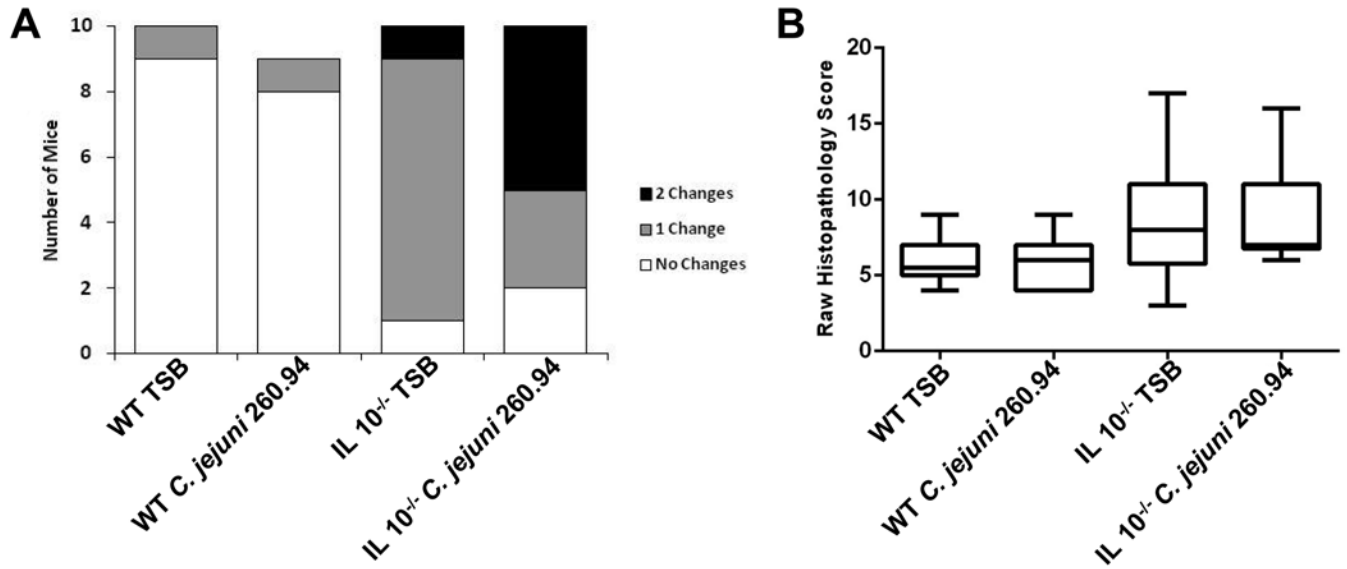

Figure 2. (A) Gross pathologic changes noted at necropsy and (B) histopathologic assessment of the ileocecocolic junction of 19 BALB/c WT and 20 BALB/c IL10$^{-/-}$ mice that received either *Campylobacter jejuni* 260.94 or vehicle control (tryptic soy broth, TSB). Mice were euthanized at 5 wk after infection. One infected WT mouse required early euthanasia unrelated to *C. jejuni* and is excluded from these data. (A) Gross lesions noted at necropsy included enlarged or thickened wall of proximal colon (present in all 17 IL10$^{-/-}$ mice with at least one change); other more sporadic changes included enlarged or thickened cecum, enlarged spleen, and enlarged ileocecocolic lymph nodes. Gross pathology scores were not significantly different between sham-inoculated and *C. jejuni* 260.94-infected IL10$^{-/-}$ mice (Fisher exact test, $P_B = 0.087$). (B) Histologic assessment of colitis in the ileocecocolic junction involved assigning a raw score (maximum, 42 points) and subsequent ranking of raw scores for statistical purposes. Whiskers span minimum to maximum values, the box extends from the 25th to 75th percentiles, and the line in the middle of the box denotes the median. Mice with scores of 9 points or lower are considered to have no colitis, whereas scores of 10 to 19 indicate mild colitis. Significance was seen overall by using both the Fisher Exact Probability test on ranked data ($P_B = 0.012$) and Kruskal–Wallis analysis of raw scores ($P = 0.0265$), but no pairwise comparisons were significant in either analysis.

Kruskal–Wallis analysis of raw scores ($P = 0.0265$), no pairwise comparisons were significant in either analysis. Overall, these data suggest that IL10$^{-/-}$ mice had mildly higher baseline levels of gross gastrointestinal pathology and histologic lesions in the ileocecocolic junction than did WT mice, attributed to spontaneous colitis in IL10$^{-/-}$ mice unrelated to *C. jejuni* infection.

Immune response to *C. jejuni* infection. Systemic (plasma) and local (colonic) immune responses to infection were measured.

Plasma antibodies. Multiple antibody isotypes reacting with *C. jejuni* and gangliosides GM1 and GD1a antigens were analyzed via an indirect ELISA format. Isotypes were chosen to reflect systemic Th1 (IgG3, IgG2a, IgG2b), Th17 (IgG2b), and Th2 (IgG1) -mediated responses.[1,3,38,59] Plasma antibody responses to *C. jejuni* are shown in Figure 3 A. Infected mice mounted primarily a Th1/Th17 response to *C. jejuni,* as shown by statistically significant increases in plasma anti-*C. jejuni* IgG2a and IgG2b levels as compared with control mice, in both WT and IL10$^{-/-}$ genotypes. The Th1-mediated IgG3 was significantly higher in *C. jejuni*-infected IL10$^{-/-}$ mice as compared with sham-inoculated mice of either WT or IL10$^{-/-}$ genotype. However, infection with *C. jejuni* did not produce significantly higher IgG3 in WT mice as compared with sham-inoculated WT mice, indicating that *C. jejuni* infection stimulated a significant IgG3 response only in IL10$^{-/-}$ mice. Th2-mediated IgG1 responses were significantly higher in both sham-inoculated and infected IL10$^{-/-}$ mice as compared with sham-inoculated WT mice. Collectively, these data indicate that BALB/c mice infected with *C. jejuni* 260.94 mounted a primary Th1/Th17 systemic response that was exacerbated by IL10 deficiency.

Because antiganglioside antibodies are a hallmark of GBS and because immunopathogenesis of GBS is thought to involve molecular mimicry between *C. jejuni* lipooligosaccharide and peripheral nerve gangliosides, we also measured anti-GM1 and anti-GD1a antibodies via ELISA. In general, magnitude of response and patterns of elevation in different groups were similar for anti-GM1 antibodies (Figure 3 B) and anti-GD1a antibodies (Figure 3 C). Significant increases in anti-GM1 and anti-GD1a IgG2b were seen in IL10$^{-/-}$ mice, with infected IL10$^{-/-}$ mice having significantly higher levels than did infected WT mice. However, antiganglioside IgG2b was not significantly different in C. *jejuni*-infected mice as compared with control mice of either genotype. Anti-GM1 IgG3 was significantly higher in sham-inoculated WT mice than in infected and control IL10$^{-/-}$ mice. Infected WT mice had significantly higher IgG3 than did sham-inoculated IL10$^{-/-}$ mice. No other significant differences were seen between groups, including in Th2-mediated IgG1 antibodies. Collectively, these data suggest that elevations in antiganglioside antibodies were more closely related to the presence or absence of IL10 rather than to *C. jejuni* infection status.

Colon cytokine production. Cytokines reflecting differentiation of Th1, Th2, Th17, Th9, Th22, and Tfh cells were measured in a panel that included IFNγ, TNFα, IL2, IL4, IL5, IL6, IL9, IL10, IL13, IL17A, IL17F, IL21, and IL22. Cytokines that were not statistically analyzed included IL5, IL17F, and IL21, of which only 1 of the 39 mice produced a detectable amount; IL10, of which only one WT mouse and no IL10$^{-/-}$ mice produced a detectable amount; and IL4 and IL13, of which no mouse of either genotype produced a detectable amount.

No significant changes related to infection status were found between the WT and IL10$^{-/-}$ genotypes for any cytokine (Figure 4). However, sham-inoculated IL10$^{-/-}$ mice produced significantly more TNFα and IFNγ than did either sham-inoculated or *C. jejuni* 260.94–infected WT mice. The overall analysis of IL17A was statistically significant (Kruskal–Wallis, $P = 0.0289$), but none of the pairwise comparisons were significantly different. Mean values of TNF-α, IFN-γ, IL-6, IL-17A, and IL-22 were

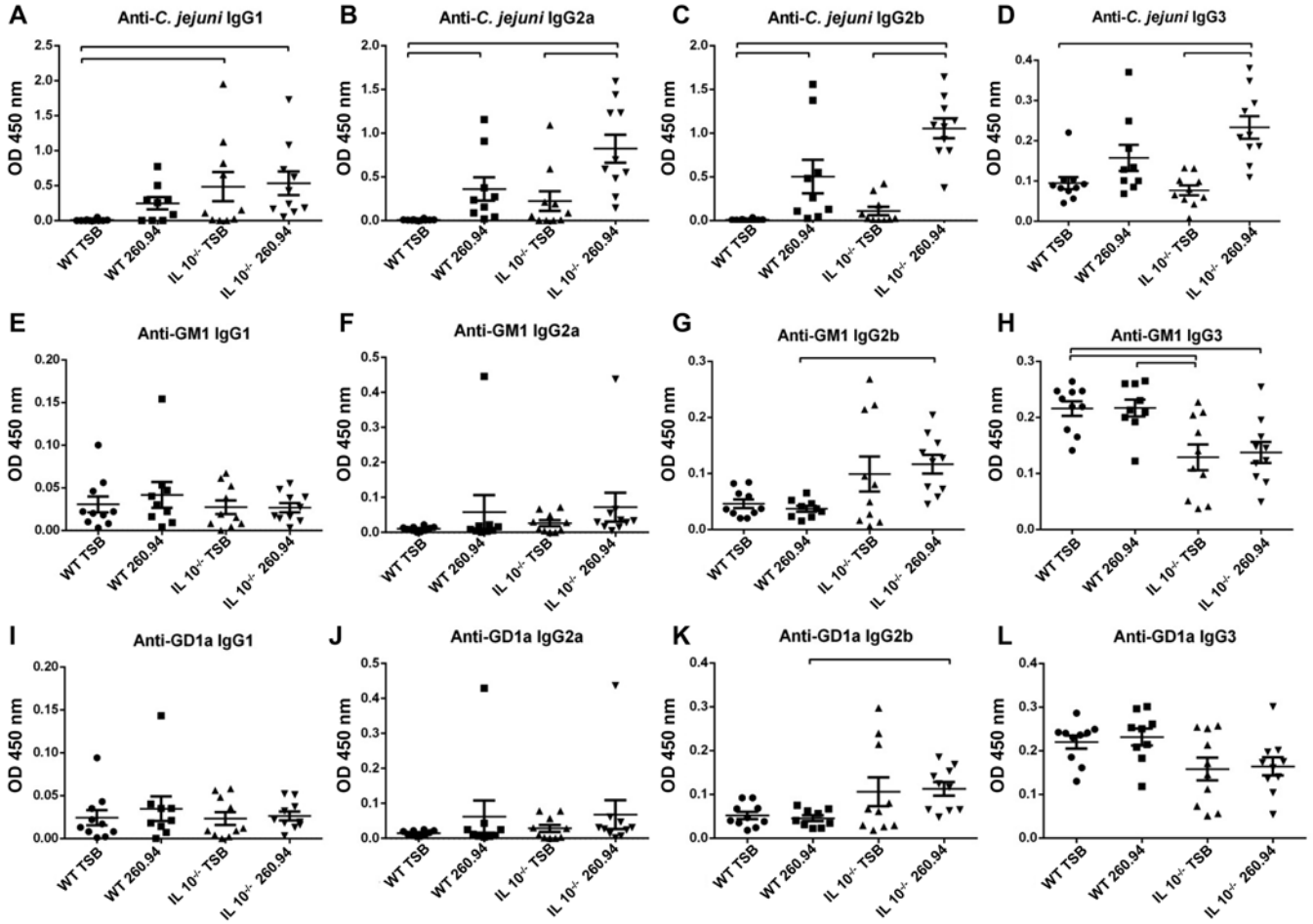

Figure 3. Quantification of plasma antibodies in experimental mice by indirect ELISA. Antibodies detected are A) Anti-*C. jejuni* IgG1, B) Anti-*C. jejuni* IgG2a, C) Anti-*C. jejuni* IgG2b, D) Anti-*C. jejuni* IgG3, E) Anti-GM1 ganglioside IgG1, F) Anti-GM1 ganglioside IgG2a, G) Anti-GM1 ganglioside IgG2b, H) Anti-GM1 ganglioside IgG3, I) Anti-GD1a ganglioside IgG1, J) Anti-GD1a ganglioside IgG2a, K) Anti-GD1 ganglioside IgG2b, L) Anti-GD1 ganglioside IgG3. BALB/c WT and IL10$^{-/-}$ mice were inoculated with either *C. jejuni* 260.94 or vehicle (tryptic soy broth, TSB) and euthanized at 5 wk after infection. One infected WT mouse required early euthanasia unrelated to *C. jejuni* and is excluded from these data. *P* values less than 0.05 were considered significant. Lines above the data (mean ± SEM) indicate significant differences between groups (Kruskal–Wallis analysis, followed by the Dunn posttest).

numerically lower in *C. jejuni* 260.94-infected IL-10$^{-/-}$ mice than in sham-inoculated IL-10$^{-/-}$ mice, but the differences were not statistically significant, Overall, these data suggest that production of cytokines reflecting Th1/Th17/Th22 differentiation may be a characteristic of IL10$^{-/-}$ mice.

Nerve histopathology. Cells positively labeled with the F4/80 macrophage marker in DRG and afferent nerve fibers were quantified by morphometry (Figure 5). *C. jejuni*-infected BALB/c IL10$^{-/-}$ mice showed the most variation in number of F4/80-positive cells, with scores ranging from 2 to 33, whereas F4/80-positive scores in sham-inoculated WT mice were the most tightly clustered (range, 5 to 18). No statistically significant differences were found between treatment groups ($P = 0.290$). These data indicate that, in this model, neither absence of IL10 nor infection with *C. jejuni* 260.94 significantly influenced macrophage numbers in DRG after 5 wk of infection.

Discussion

The aim of the current study was to develop a mouse model of GBS subsequent to *C. jejuni* infection, to further our understanding of the complex immunopathogenesis of this important human disease. The model aimed to exploit the reported Th2 bias of BALB/c mice; in the absence of antiinflammatory IL10, these mice were expected to mount strong Th2-mediated immunity after infection with GBS patient-derived *C. jejuni* 260.94, which harbors a GM1a ganglioside mimic.[33] We expected the production of antiganglioside antibodies and associated nerve lesions, as had been reported for C57BL/6 IL10$^{-/-}$ and WT, B7-2$^{-/-}$, and IL10$^{-/-}$ NOD mice infected with *C. jejuni* 260.94.[35,55] Instead, our WT and IL10$^{-/-}$ BALB/c mice orally inoculated with *C. jejuni* 260.94 mounted primarily Th1/Th17 immune responses and did not develop colitis, antiganglioside antibody production, an overt neurologic phenotype, or nerve lesions. When considered in the context of previously published models from our group using various combinations of mouse and *C. jejuni* strains,[4,35,36,55] the current study further highlights the importance of both the characteristics of the infecting *C. jejuni* strain (e.g., presence of ganglioside mimics, invasiveness, colitogenic potential) and host factors (genetic background, immunologic biases) in determining disease outcome.

Our first hypothesis was that Th2-mediated immune responses, including the production of antiganglioside antibodies but without induction of colitis, would predominate after oral inoculation of WT and IL10$^{-/-}$ BALB/c mice with *C. jejuni*

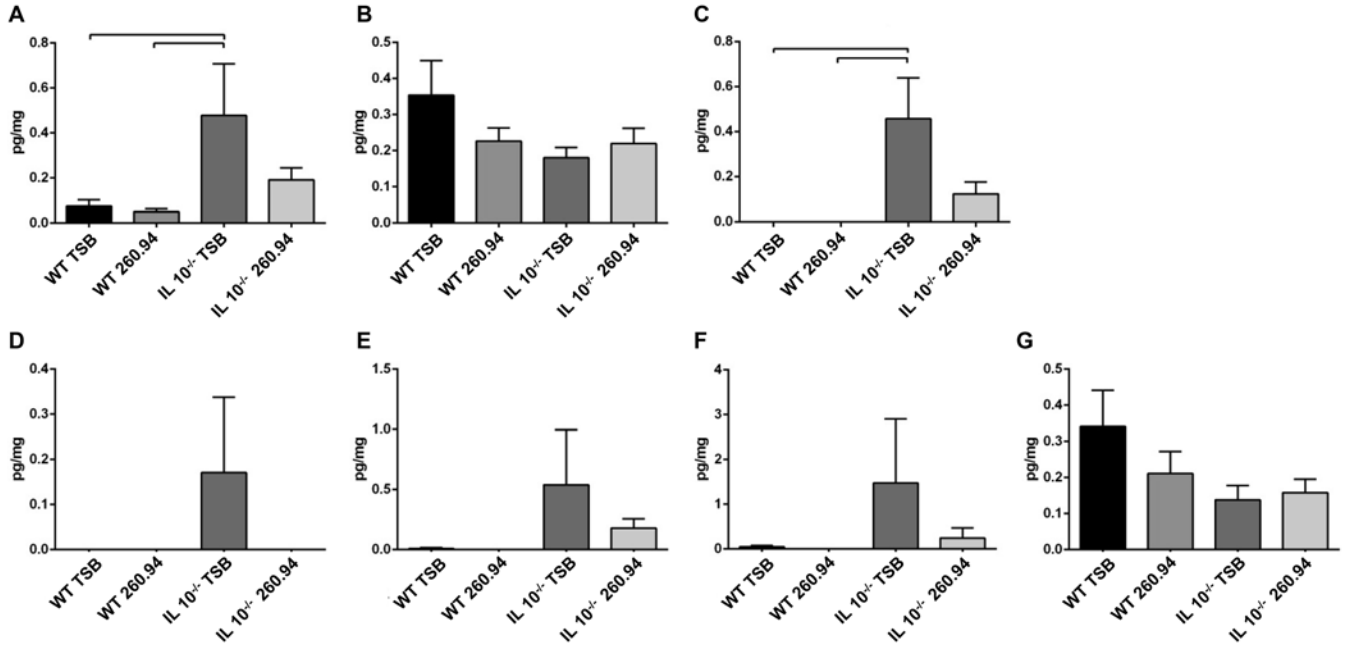

Figure 4. Cytokine production, presented as picograms of cytokine per milligram of colonic tissue, was measured in supernatants of homogenized colon samples by using a flow cytometry-based multiplex bead array. Panels show A) TNFα, B) IL2, C) IFNγ, D) IL6, E) IL17A, F) IL22, and G) IL9 cytokines. Treatment groups included WT and IL10$^{-/-}$ BALB/c mice, either sham-inoculated (tryptic soy broth, TSB) or orally infected with *C. jejuni* 260.94. Mice were euthanized at 5 wk after infection. The one infected WT mouse requiring early euthanasia unrelated to *C. jejuni* is excluded. *P* values less than 0.05 were considered significant. Lines above data (mean ± SEM) indicate significant differences (Kruskal–Wallis ANOVA on ranks, followed by the Dunn posttest). Overall significance was found in analysis of IL17A ($P = 0.0289$), although no pairwise comparisons were significant.

260.94. This reasoning was based on reports in the literature of a relative Th2 bias exhibited by BALB/c mice in comparison with other mouse strains, including C57BL/6 mice, in both in vivo infection models and in vitro studies,[33,39,49] and the Th2-mediated response shown in C57BL/6 IL10$^{-/-}$ mice infected with *C. jejuni* 260.94.[35] Instead, infected WT and IL10$^{-/-}$ BALB/c mice responded with significantly increased *C. jejuni*-specific plasma antibodies including IgG2a, IgG2b, and IgG3 antibody isotypes but without significantly increased IgG1 production related to infection (Figure 3), indicating Th1/Th17-mediated class switching.[1,3,59] This unexpected result offers deeper insight into the diverse regulatory actions of IL10 and the interplay of infecting pathogen and immunologic bias of the host genetic background. Although C57BL/6 and BALB/c mice reportedly exhibit Th1- and Th2-mediated immune biases, respectively, the current study and others demonstrate that characteristics of the infecting pathogen or stimulus contribute substantially to immunologic outcomes. C57BL/6 and C.B-17 (a BALB/c strain congenic for the C57BL/6 Ig heavy-chain gene segment) mice infected with *Cryptococcus neoformans*, a fungal lung mucosal pathogen, showed differing immune responses and ability to clear the pathogen: susceptible C57BL/6 mice exhibited increasing lung burden over time, whereas resistant C.B-17 mice mounted an early and local Th1-mediated response that correlated with superior pathogen clearance.[23] BALB/c mice are resistant to developing chemically induced (i.e., dextran sulfate sodium) colitis, whereas C57BL/6 mice are susceptible.[63] Assessment of cytokine production after exposure to DSS indicates that BALB/c mice exhibit Th2/Th17/Treg-mediated responses, characterized by the production of IL4, IL6, IL10, and IL17 and higher numbers of Treg cells in the regional lymph node, whereas C57BL/6 mice respond with strong IFNγ production.[63] C. *jejuni* is a mucosal enteric pathogen and elicits a Th1/Th17-mediated response in most in vivo and in vitro mouse and ex vivo human *C. jejuni* infection studies.[4,16,17,35,36,47,55] Therefore, WT BALB/c mice may be predisposed to Th2 responses to some challenges, but the current study suggests that Th1/Th17 responses are predominant in BALB/c mice after *C. jejuni* infection, even with a *C. jejuni* strain that previously induced Th2 responses in C57BL/6 IL10$^{-/-}$ mice.[35] Th1/Th17 responses were more robust in IL10$^{-/-}$ mice, but because a similar pattern was observed in WT mice, the absence of IL10 and subsequent enhancement of Th1-mediated immunity cannot be the sole reason for this outcome. These results further highlight the complexity of GBS immunopathogenesis and the interplay of both host and pathogen characteristics in the induction of immunity.

The induction of antiganglioside antibodies is a hallmark of GBS and a partial reflection of the immune response to *C. jejuni* infection. We expected that infected WT and IL10$^{-/-}$ BALB/c mice would produce antibodies to GM1 and GD1a gangliosides, as previously reported in other mouse genotypes.[9,35,55] In the current study, Th1/Th17-mediated IgG2b and IgG3 isotypes reacting with GM1 and GD1a antigens showed significant elevations related only to presence or absence of IL10 (Figure 3) but not to *C. jejuni* infection status. The primary Th1/Th17 response, as opposed to a primary Th2-mediated response, apparently does not preclude generation of antiganglioside antibodies: in a separate study, BALB/c IL10$^{-/-}$ mice infected with the enteritis-associated *C. jejuni* 11168 strain developed severe colitis, marked local and systemic Th1/Th17-mediated immunity, and anti-GM1 and anti-GD1a antibodies.[10] Therefore, the possibility that severe colitis or strong local colonic adaptive immune responses are required for generation of antiganglioside antibodies in some models cannot be excluded. Another possibility is that IL10-mediated host–microbiota interactions influence antiganglioside antibody production in response to ganglioside mimics expressed by commensal flora, but additional studies would be necessary to establish such a connection.

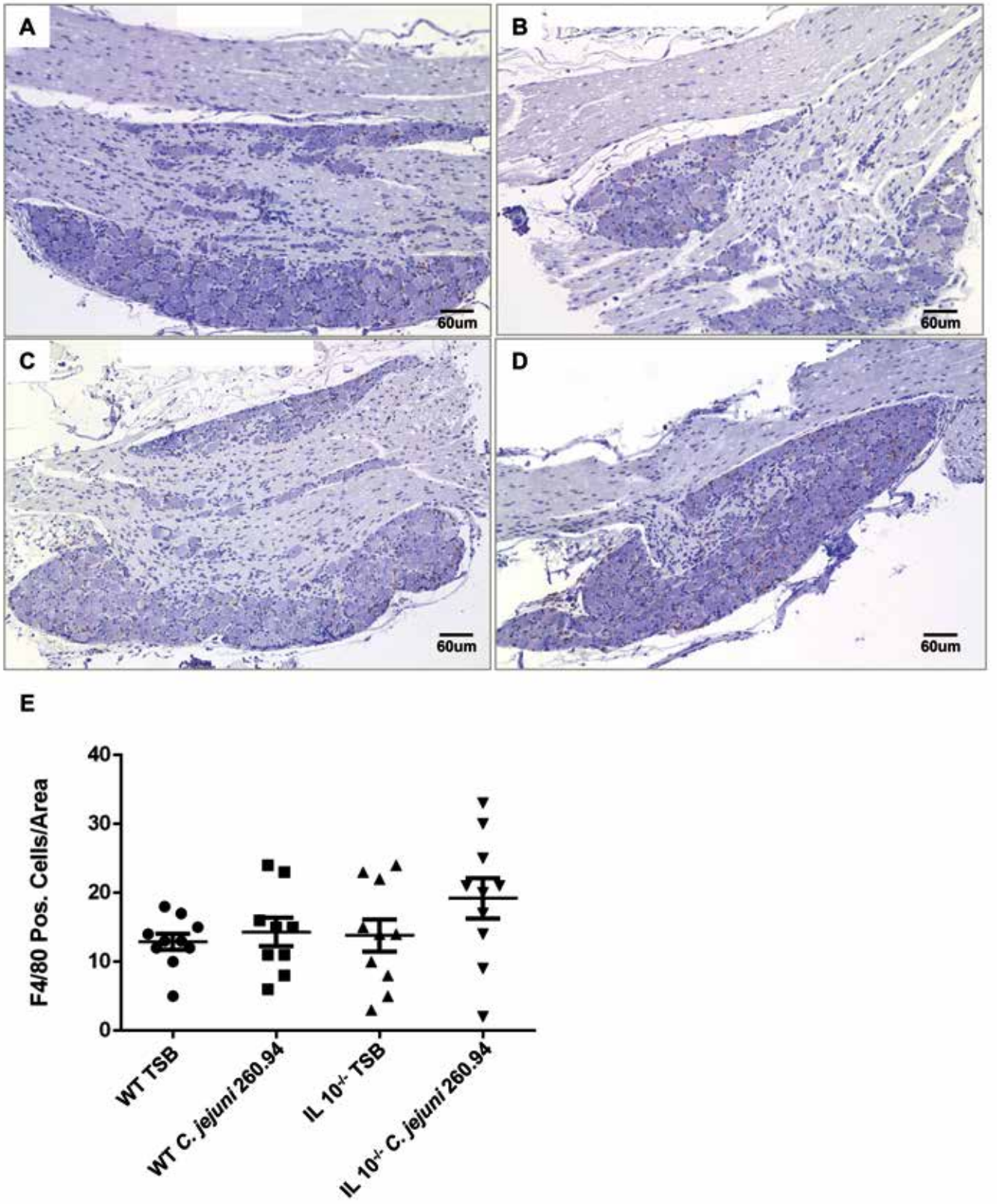

Figure 5. Macrophages in lumbar dorsal root ganglia (DRG) dissected from 19 BALB/c WT and 20 BALB/c IL10$^{-/-}$ mice given either *C. jejuni* 260.94 or TSB (sham; tryptic soy broth). Panels show representative sections from groups A) BALB/c TSB, B) BALB/c *C. jejuni* 260.94, C) BALB/c IL 10$^{-/-}$ TSB, and D) BALB/c IL 10$^{-/-}$ *C. jejuni* 260.94. Panel E graph shows positive F4/80-stained cells from the dorsal root ganglia of the four groups of mice. Mice were euthanized at 5 wk after infection. Macrophages identified by immunohistochemical labeling with F4/80 were quantitatively scored by using morphometry in Image J. Results are given as the number (mean ± SEM) of F4/80-positive cells per unit area (100,000 pixels). No significant differences between groups were seen (Kruskal–Wallis, $P = 0.290$). Bar, 60 µm.

Data from the current study showed similar patterns of anti-GM1 and anti-GD1a antibody production. *C. jejuni* 260.94 is reported to harbor a GM1a mimic but apparently not other ganglioside mimics.[34] Similar patterns of production of anti-GM1 and anti-GD1a antibodies were also reported in a study involving *C. jejuni* 11168,[10] which reportedly does not possess GD1a mimics.[34] GM1 and GD1a gangliosides are extremely similar in structure,[2] and the possibility that the plasma antibodies directed at GM1 also bound GD1a antigen in the ELISA should be considered. In addition, the lipooligosaccharide of *C. jejuni* strain 81–176 possesses structures mimicking several gangliosides, and phase variation can change the expression of ganglioside mimics.[19] Therefore, the possibility that *C. jejuni* or commensal flora can express different or multiple ganglioside mimics in vivo, resulting in generation of more than one type of antiganglioside antibody, cannot be excluded.

Despite persistent colonization of 90% of infected mice at the end of the 5-wk study, neither gross pathology nor histologic changes in the ileocecocolic junction were significantly increased in either WT or IL10$^{-/-}$ mice as compared with sham-inoculated mice (Figure 2). A higher baseline of overall mild colitis in IL10$^{-/-}$ mice regardless of *C. jejuni* infection status likely reflects the development of spontaneous colitis in IL10$^{-/-}$ mice due to unchecked responses to the intestinal microbiota.[6,29] In addition, uncontrolled immune responses to enteric antigens may explain (at least in part) the presence of *C. jejuni*-specific plasma IgG1 and IgG2a in some sham-inoculated IL10$^{-/-}$ mice (Figure 3); all sham-inoculated mice were negative for *C. jejuni* by both culture and PCR analysis, and the positive *C. jejuni* plasma response may reflect generation of antibodies against a structurally similar antigen in the microbiota. Colitis can occur in IL10$^{-/-}$ mice at as early as 3 to 4 wk of age,[6,29] and the mice in the current study were inoculated at 14 to 15 wk of age and euthanized at 5 wk after inoculation. Therefore, we attribute the mild pathology in our IL10$^{-/-}$ mice to spontaneous disease and not to *C. jejuni* infection. The relatively later age at inoculation in the current study as compared with other studies was chosen to allow the mice to increase in body size prior to intragastric gavage. Results of the current study are consistent with other mouse models demonstrating lack of colitis despite high colonization rates after infection with *C. jejuni* 260.94.[4,9,35,55] *C. jejuni* strains vary widely in ability to colonize and cause colitis, with pathogenicity related to genomic content of certain open reading frames,[4] and even in IL10$^{-/-}$ mice *C. jejuni* 260.94 has not been colitogenic in our models.

C. jejuni-specific plasma antibody isotypes reflected a systemic Th1/Th17 response in infected mice, but a significant local adaptive immune response was not identified in the proximal colon (Figure 4). Consistent with a shift toward Th1-mediated immunity in the absence of IL10 and infection with a mucosal enteric pathogen, the production of Th2 cytokines—including IL4, IL5, and IL13—was virtually undetectable. Significant increases were identified only in TNFα and IFNγ production in sham-inoculated IL10$^{-/-}$ mice compared with WT mice, reflecting the Th1-mediated spontaneous colitis occurring in IL10$^{-/-}$ mice. No significant difference in production of any cytokine by either WT or IL10$^{-/-}$ mice was related to infection.

The second aim of the current study was to determine whether *C. jejuni* 260.94 infection leads to neuropathology—manifested by gait abnormalities, neuromuscular weakness, and macrophage infiltration into DRG—in BALB/c mice. To determine neurologic deficits, we performed 3 vigorous phenotyping tests prior to inoculation and weekly thereafter until euthanasia at 5 wk. Of these tests, the DigiGait treadmill analyses were most informative (Table 1). Two-way repeated-measures ANOVA revealed numerous significant differences in variables with time, most of which included baseline compared with 4 wk after inoculation. The only variable exhibiting significant differences related to infection status when all treatment groups were analyzed together was forelimb stance width, with infected IL10$^{-/-}$ mice having a wider stance than sham-inoculated WT mice. The difference in stance width between infected and sham-inoculated mice remained significant when WT mice were analyzed separately but was insignificant within IL10$^{-/-}$ mice. The wider stance width could indirectly reflect hindlimb weakness, with more body weight being front-loaded to compensate, leading to wider stance width in the front. The DigiGait system is designed to detect subtle gait changes, but this single change is difficult to interpret without other concurrent gait disturbances to clarify its significance.

The hang test and OFT were not informative in the current study. The hang test was used as a measure of motor strength and balance. Significant differences determined by 2-way repeated measures ANOVA were related to time but not infection status. Subjective observations suggest that, in the current study, this test likely was inadequate for detecting neurologic deficits. More active mice tended to move around more on the grid, leading to a shorter hang time that was unrelated to weakness. In contrast, some mice tended to hook their feet through the bars and hang on until the end of the test period. These observations suggest that for BALB/c mice, the hang test performed with this technique did not reflect motor deficits but instead activity level and was thus not a useful neurologic indicator. Similarly, recordings of the OFT—in which mice were placed in a standard rat cage to observe gait, movement, and posture—were not analyzed because the mice did not consistently exhibit sufficient spontaneous movement to allow meaningful observation. Less movement and rearing by BALB/c mice as compared with other mouse strains has been reported previously for the OFT[12,30] and may be related to photophobia in albinos, such as BALB/c mice.[13] Despite the disadvantages of the OFT and hang test, the 3 neurologic phenotyping tests combined with careful daily observation should have revealed an overt neurologic phenotype, had one been present. Considering all of these findings, we conclude that infection with GBS patient-derived *C. jejuni* 260.94 did not lead to neurologic deficits in the current study.

Neuropathology was assessed by evaluation of macrophage numbers in lumbar DRG and their afferent nerve fibers. We chose macrophages as indicators of neuropathology due to their postulated role in GBS pathogenesis, particularly in the acute motor axonal form of GBS, which some consider to be the subtype most closely associated with preceding *C. jejuni* infection.[15,41,57] We also chose DRG for assessment, because GBS patients frequently describe pain and sensory defects.[57] Cell bodies of sensory fibers reside in the DRG, which are also reported to have a particularly leaky blood-nerve barrier that predisposes this area to immune-mediated damage.[41] Pathology in dorsal roots has been described in the autopsies of patients succumbing to the motor-sensory axonal form of GBS,[18] and increased numbers of F4/80-positive cells were present mainly in the DRG, with fewer in the sciatic nerve or brachial plexus, of NOD and NOD IL10$^{-/-}$ mice infected with *C. jejuni* 260.94.[55]

Taken together with other studies,[9,35,55] the current study in BALB/c mice further indicates that the immunopathogenesis of nerve damage in GBS is incompletely understood. Despite significantly elevated antiganglioside GM1 and GD1a IgG2b and IgG3 antibodies in the plasma of *C. jejuni* 260.94-infected BALB/c mice (Figure 3), no significant increases were found in the

number of F4/80-positive cells in lumbar DRG and their afferent nerve fibers and no detectable defects were found in the DRG (Figure 5). *C. jejuni* 260.94-infected C57BL/6 mice with a human gut microbiota similarly demonstrated few F4/80-positive cells in sciatic nerves and DRG, even though they had significantly elevated anti-GM1 IgG1.[9] However, in another model developed by our group, NOD *C. jejuni* 260.94-infected mice exhibited the onset of nerve lesions at 5 wk after inoculation.[55] In that study, both NOD and NOD IL10$^{-/-}$ *C. jejuni* 260.94-infected mice had GBS lesions in the DRG and afferent nerve fibers 4 to 6 wk after infection, whereas uninfected controls did not, and lesions were seen only in mice with higher anti-GM1 or anti-GD1a antibody levels.[55] The lack of increased macrophages in DRG and afferent nerve fibers in infected BALB/c mice, despite significantly higher plasma antiganglioside antibodies in some groups, suggests that antiganglioside antibodies alone are not sufficient to cause nerve lesions mediated by macrophages in DRG. The gut microbiome may influence GBS onset. Bacteria other than *C. jejuni* possess GM1 gangliosides that could produce molecular mimicry.[43] These organisms may play an important role in GBS development, causing immune-mediated tolerance or training toward the ganglioside antigen. We acknowledge that labeling of other immune components implicated in nerve damage in GBS, such as T cells, complement, and IgG[41,57] in peripheral nerve tissues and conducting a time-course study to determine whether and when neuropathology is correlated with antiganglioside antibody production, would provide a more complete assessment of GBS immunopathogenesis. Regardless, when taken together, the data regarding the absence of neurologic deficits identified by rigorous phenotyping tests—including DigiGait treadmill analysis, OFT, and hang testing—and the lack of increased macrophages in DRG indicate that neuropathology was not induced by *C. jejuni* 260.94 in BALB/c WT or IL10$^{-/-}$ mice in the current study.

The final aim of this study was to determine whether the absence of the regulatory actions of IL10 resulted in exacerbation of immune responses and neuropathology. The systemic Th1/Th17 immune response to *C. jejuni* 260.94, manifested by significant increases in *C. jejuni*-specific IgG2a, IgG2b, and IgG3 antibody isotypes, was greater in magnitude in IL10$^{-/-}$ compared with WT BALB/c mice (Figure 3). Furthermore, *C. jejuni* induced significant IgG3 production only in the IL10$^{-/-}$ group. Therefore, the absence of IL10 enhanced systemic Th1/Th17 immunity in *C. jejuni* infected mice in this model.

The presence or absence of IL10 led to differences in antiganglioside antibody production, and the absence of IL10 was associated with mild colitis and increased production of specific cytokines in the colon. However, IL10 deficiency did not lead to significant exacerbation of *C. jejuni*-induced changes in immunity or neuropathology. No significant difference in cecal *C. jejuni* colonization was found between WT and IL10$^{-/-}$ mice. Equal numbers of sham-inoculated and infected IL10$^{-/-}$ mice developed mild colitis with similar histologic lesions, indicating that IL10$^{-/-}$ mice had underlying spontaneous colitis that was not exacerbated by *C. jejuni* infection. Similarly, the production of TNFα and IFNγ in the proximal colon was increased overall in IL10$^{-/-}$ mice, but no significant differences were seen related to *C. jejuni* infection. Therefore, in this model, synergism between *C. jejuni* infection and IL10 deficiency that resulted in increased pathology or neurologic deficits was not observed.

Results of this study indicate that WT and IL10$^{-/-}$ BALB/c mice orally inoculated with GBS patient–derived *C. jejuni* 260.94 are stably colonized, mount systemic Th1/Th17 responses, and do not develop colitis, produce antiganglioside antibodies, or develop neuropathology, including neurologic deficits and inflammatory lesions in DRG. Systemic Th1/Th17-mediated immunity was unexpected, considering the reported Th2 immunologic bias in BALB/c mice and the previous induction of Th2-mediated immunity in C57BL/6 IL10$^{-/-}$ mice infected with *C. jejuni* 260.94.[35] These results indicate BALB/c mice are a useful model for studying *C. jejuni* infection and could provide critical insights into the influence of host genetic background in the polarization of the immune response and resulting pathology.

Acknowledgments

These studies were funded with federal funds from the National Institute of Allergy and Infectious Disease, NIH, Department of Health and Human Services, under grant number U19AI090872, Enterics Research Investigational Network, Cooperative Research Center, and the NCRR, NIH, Department of Health and Human Services, under grant number 5K26RR023080. Jean M Brudvig was supported for 6 semesters by a fellowship grant from the College of Veterinary Medicine, Michigan State University. Student salaries and Dr Mansfield's salary were supported by funds from the Albert C and Lois E Dehn Endowment in Large Animal Clinical Sciences, College of Veterinary Medicine, and NC1202 Multistate projects funds from the USDA.

All applicable international, national, and/or institutional guidelines for the care and use of animals were followed.

References

1. **Abbas AK, Murphy KM, Sher A.** 1996. Functional diversity of helper T lymphocytes. Nature **383:**787–793. https://doi.org/10.1038/383787a0.
2. **Ang CW, Laman JD, Willison HJ, Wagner ER, Endtz HP, DeKlerk MA, Tio-Gillen AP, Van den Braak N, Jacobs BC, Van Doorn PA.** 2002. Structure of *Campylobacter jejuni* lipopolysaccharides determines antiganglioside specificity and clinical features of Guillain–Barre and Miller–Fisher patients. Infect Immun **70:**1202–1208. https://doi.org/10.1128/IAI.70.3.1202-1208.2002.
3. **Bai Y, Liu R, Huang D, La Cava A, Tang Y, Iwakura Y, Campagnolo DI, Vollmer TL, Ransohoff RM, Shi F-D.** 2008. CCL2 recruitment of IL6-producing CD11b+ monocytes to the draining lymph nodes during the initiation of Th17-dependent B cell-mediated autoimmunity. Eur J Immunol **38:**1877–1888. https://doi.org/10.1002/eji.200737973.
4. **Bell JA, Jerome JP, Plovanich-Jones AE, Smith EJ, Gettings JR, Kim HY, Landgraf JR, Lefebure T, Klopper JJ, Rathinam VA, St. Charles JL, Buffa BA, Brooks AP, Poe SA, Eaton KA, Stanhope MJ, Mansfield LS.** 2013. Outcome of infection of C57BL/6 IL10$^{-/-}$ mice with *Campylobacter jejuni* strains is correlated with genome content of open reading frames up- and downregulated in vivo. Microb Pathog **54:**1–19. https://doi.org/10.1016/j.micpath.2012.08.001.
5. **Bereswill S, Fischer A, Plickert R, Haag L-M, Ott, B, Kuhl AA, Dashti JI, Zautner AE, Munoz M, Loddenkemper C, Grob U, Gobel UB, Heimesaat MM.** 2011. Novel murine infection models provide deep insights into the "menage a trois" of *Campylobacter jejuni*, microbiota and host innate immunity. PLoS One **6:**e20953. https://doi.org/10.1371/journal.pone.0020953.
6. **Berg DJ, Davidson N, Kuhn R, Muller W, Menon S, Holland G, Thompson-Snipes L, Leach MW, Rennick D.** 1996. Enterocolitis and colon cancer in interleukin-10-deficient mice are associated with aberrant cytokine production and CD4(+) TH1-like responses. J Clin Invest **98:**1010–1020. https://doi.org/10.1172/JCI118861.
7. **Berndtson E, Danielsson-Tham ML, Engvall A.** 1994. Experimental colonization of mice with *Campylobacter jejuni*. Vet Microbiol **41:**183–188. https://doi.org/10.1016/0378-1135(94)90147-3.
8. **Blaser MJ, Duncan DJ, Warren GH, Wang WL.** 1983. Experimental *Campylobacter jejuni* infection of adult mice. Infect Immun **39:**908–916. https://doi.org/10.1128/iai.39.2.908-916.1983.
9. **Brooks PT, Brakel KA, Bell JA, Bejeck CE, Gilpin T, Brudvig JM, Mansfield LA.** 2017. Transplanted human fecal microbiota enhanced Guillain Barre syndrome autoantibody responses after *Campylobacter jejuni* infection in C57BL/6 mice. Microbiome **5:**92. https://doi.org/10.1186/s40168-017-0284-4.

10. **Brudvig JM**. 2018. Infecting *Campylobacter jejuni* strain determines TH1/TH17-mediated immunity and colitis in interleukin-10-deficient BALB/C mice, p 90–151. In: Brudwig JM, editor. Interplay of host and pathogen factors determines immunity and clinical outcome following Campylobacter jejuni infection in mice. East Lansing (MI): Michigan State University.
11. **Chang C, Miller JF.** 2006. *Campylobacter jejuni* colonization of mice with limited enteric flora. Infect Immun **74:**5261–5271. https://doi.org/10.1128/IAI.01094-05.
12. **Crawley JN.** 2007. What's wrong with my mouse?: behavioral phenotyping of transgenic and knockout mice. 2nd ed. Hoboken (NJ): John Wiley & Sons, Inc. https://doi.org/10.1002/0470119055
13. **DeFries JC, Hegmann JP, Weir MW.** 1966. Open-field behavior in mice: evidence for a major gene effect mediated by the visual system. Science **154:**1577–1579. https://doi.org/10.1126/science.154.3756.1577.
14. **Dorman CW, Krug HE, Frizelle SP, Funkenbusch S, Mahowald ML.** 2013. A comparison of DigiGait and TreadScan imaging systems: assessment of pain using gait analysis in murine monoarthritis. J Pain Res **7:**25–35.
15. **Drenthen J, Yuki N, Meulstee J, Maathuis EM, van Doorn PA, Visser GH, Blok JH, Jacobs BC.** 2011. Guillain-Barre syndrome subtypes related to *Campylobacter* infection. J Neurol Neurosurg Psychiatry **82:**300–305. https://doi.org/10.1136/jnnp.2010.226639.
16. **Edwards LA, Nistala K, Mills DC, Stephenson HN, Zilbauer M, Wren BW, Dorrell N, Lindley KJ, Wedderburn LR, Bajaj-Elliott M.** 2010. Delineation of the innate and adaptive T-cell immune outcome in the human host in response to *Campylobacter jejuni* infection. PLoS One **5:**e15398. https://doi.org/10.1371/journal.pone.0015398.
17. **Fox JG, Rogers AB, Whary MT, Ge Z, Taylor NS, Xu S, Horwitz BH, Erdman SE.** 2004. Gastroenteritis in NF-kappaB-deficient mice is produced with wild-type *Camplyobacter jejuni* but not with C. jejuni lacking cytolethal distending toxin despite persistent colonization with both strains. Infect Immun **72:**1116–1125. https://doi.org/10.1128/IAI.72.2.1116-1125.2004.
18. **Griffin JW, Li CY, Ho TW, Tian M, Gao CY, Xue P, Mishu B, Cornblath DR, Macko C, McKhann GM, Asbury AK.** 1996. Pathology of the motor-sensory axonal Guillain-Barre syndrome. Ann Neurol **39:**17–28. https://doi.org/10.1002/ana.410390105.
19. **Guerry P, Szymanski CM, Prendergast MM, Hickey TE, Ewing CP, Pattarini DL, Moran, AP.** 2002. Phase variation of *Campylobacter jejuni* 81-176 lipooligosaccharide affects ganglioside mimicry and invasiveness in vitro. Infect Immun **70:**787–793. https://doi.org/10.1128/IAI.70.2.787-793.2002.
20. **Hadden RDM, Karch H, Hartung HP, Zielasek J, Weissbrich B, Schubert J, Weishaupt A, Cornblath DR, Swan AV, Hughes RAC, Toyka KV.** 2001. Preceding infections, immune factors, and outcome in Guillain-Barre syndrome. Neurology **56:**758–765. https://doi.org/10.1212/WNL.56.6.758.
21. **Halstead SK, Zitman FM, Humphreys PD, Greenshields K, Verschuuren JJ, Jacobs BC, Rother RP, Plomp JJ, Willison HJ.** 2008. Eculizumab prevents antiganglioside antibody-mediated neuropathy in a murine model. Brain **131:**1197–1208. https://doi.org/10.1093/brain/awm316.
22. **Hansen ST, Pulst SM.** 2013. Response to ethanol induced ataxia between C57BL/6J and 129X1/SvJ mouse strains using a treadmill-based assay. Pharmacol Biochem Behav **103:**582–588. https://doi.org/10.1016/j.pbb.2012.10.010.
23. **Hoag KA, Street NE, Huffnagle GB, Lipscomb MF.** 1995. Early cytokine production in pulmonary Cryptococcus neoformans infections distinguishes susceptible and resistant mice. Am J Respir Cell Mol Biol **13:**487–495. https://doi.org/10.1165/ajrcmb.13.4.7546779.
24. **Jacobs BC, Hazenberg MP, van Doorn PA, Endtz HP, van der Meche FG.** 1997. Cross-reactive antibodies against gangliosides and *Campylobacter jejuni* lipopolysaccharides in patients with Guillain-Barre or Miller Fisher syndrome. J Infect Dis **175:**729–733. https://doi.org/10.1093/infdis/175.3.729.
25. **Jacobs BC, Koga M, van Rijs W, van Doorn PA, Willison HJ, Yuki N.** 2008. Subclass IgG to motor gangliosides related to infection and clinical course in Guillain-Barre syndrome. J Neuroimmunol **194:**181–190. https://doi.org/10.1016/j.jneuroim.2007.11.017.
26. **Jacobs BC, Rothbarth PH, van der Meche FGA,,Herbrink P, Schmitz PIM, de Klerk MA, van Doorn PA**.1998. The spectrum of antecedent infections in Guillain-Barre syndrome: a case-control study. Neurology **51:**1110–1115. https://doi.org/10.1212/WNL.51.4.1110.
27. **Keithlin J, Sargeant J, Thomas MK, Fazil A.** 2014. Systematic review and meta-analysis of the proportion of *Campylobacter* cases that develop chronic sequelae. BMC Public Health **14:**1203. https://doi.org/10.1186/1471-2458-14-1203.
28. **Koga M, Yuki N, Hirata K, Morimatsu M, Mori M, Kuwabara S.** 2003. Anti-GM1 antibody IgG subclass: a clinical recovery predictor in Guillain-Barre syndrome. Neurology **60:**1514–1518. https://doi.org/10.1212/01.WNL.0000061615.77865.83.
29. **Kühn R, Löhler J, Rennick D, Rajewsky K, Müller W.** 1993. Interleukin-10-deficient mice develop chronic enterocolitis. Cell **75:**263–274. https://doi.org/10.1016/0092-8674(93)80068-P.
30. **Lalonde R, Strazielle C.** 2008. Relations between open-field, elevated plus-maze, and emergence tests as displayed by C57/BL6J and BALB/c mice. J Neurosci Methods **171:**48–52. https://doi.org/10.1016/j.jneumeth.2008.02.003.
31. **Li CY, Xue P, Tian WQ, Liu RC, Yang C.** 1996. Experimental *Campylobacter jejuni* infection in the chicken: an animal model of axonal Guillain-Barre syndrome. J Neurol Neurosurg Psychiatry **61:**279–284. https://doi.org/10.1136/jnnp.61.3.279.
32. **Liu T, Matsuguchi T, Tsuboi N, Yajima T, Yoshikai Y.** 2002. Differences in expression of toll-like receptors and their reactivities in dendritic cells in BALB/c and C57BL/6 mice. Infect Immun **70:**6638–6645. https://doi.org/10.1128/IAI.70.12.6638-6645.2002.
33. **Liu T, Nishimura H, Matsuguchi T, Yoshikai Y.** 2000. Differences in interleukin-12 and -15 production by dendritic cells at the early stage of *Listeria* monocytogenes infection between BALB/c and C57 BL/6 mice. Cell Immunol **202:**31–40. https://doi.org/10.1006/cimm.2000.1644.
34. **Louwen R, Horst-Kreft D, de Boer AG, van der Graaf L, de Knegt G, Hamersma M, Heikema AP, Timms AR, Jacobs BC, Wagenaar JA, Edntz HP, van der Oost J, Wells JM, Nieuwenhuis ES, van Vliet AM, Willemsen PJ, van Baarlen P, van Belkum P.** 2013. A novel link between *Campylobacter jejuni* bacteriophage defence, virulence and Guillain-Barre syndrome. Eur J Clin Microbiol Infect Dis 32(2):207-226.
35. **Malik A, Sharma D, St Charles J, Dybas LA, Mansfield LS.** 2013. Contrasting immune responses mediate *Campylobacter jejuni*-induced colitis and autoimmunity. Mucosal Immunol **7:**802–817. https://doi.org/10.1038/mi.2013.97.
36. **Mansfield LS, Bell JA, Wilson DL, Murphy AJ, Elsheikha HM, Rathinam VAK, Fierro BR, Linz JE, Young VB.** 2007. C57BL/6 and congenic interleukin-10-deficient mice can serve as models of *Campylobacter jejuni* colonization and enteritis. Infect Immun **75:**1099–1115. https://doi.org/10.1128/IAI.00833-06.
37. **Mansfield LS, Patterson JS, Fierro BR, Murphy AJ, Rathinam VA, Kopper JJ, Barbu NI, Onifade TJ, Bell JA.** 2008. Genetic background of IL10(−/−) mice alters host-pathogen interactions with *Campylobacter jejuni* and influences disease phenotype. Microb Pathog **45:**241–257. https://doi.org/10.1016/j.micpath.2008.05.010.
38. **Martin RM, Brady JL, Lew AM.** 1998. The need for IgG2c specific antiserum when isotyping antibodies from C57BL/6 and NOD mice. J Immunol Methods **212:**187–192. https://doi.org/10.1016/S0022-1759(98)00015-5.
39. **Mills CD, Kincaid K, Alt JM, Heilman MJ, Hill AM.** 2000. M-1/M-2 macrophages and the Th1/Th2 paradigm. J Immunol **164:**6166–6173. https://doi.org/10.4049/jimmunol.164.12.6166.
40. **Moran AP, Annuk H, Prendergast MM.** 2005. Antibodies induced by ganglioside-mimicking *Campylobacter jejuni* lipooligosaccharides recognise epitopes at the nodes of Ranvier. J Neuroimmunol **165:**179–185. https://doi.org/10.1016/j.jneuroim.2005.04.013.
41. **Nachamkin I, Allos BM, Ho T.** 1998. *Campylobacter* species and Guillain-Barre syndrome. Clin Microbiol Rev **11:**555–567. https://doi.org/10.1128/CMR.11.3.555.
42. **Nyati KK, Prasad KN, Kharwar NK, Soni P, Husain N, Agrawal V, Jain AK.** 2011. Immunopathology and Th1/Th2 immune response of *Campylobacter jejuni*-induced paralysis resembling Guillain-Barre syndrome in chicken. Med Microbiol Immunol (Berl) **201:**177–187. https://doi.org/10.1007/s00430-011-0220-3.

43. **Patry RT, Stahl M, Perez-Munoz ME, Nothaft H, Wenzel CQ, Sacher JC, Coros C, Walter J, Vallance BA, Szymanksi CM.** 2019. Bacterial AB5 toxins inhibit the growth of gut bacteria by targeting ganglioside-like glycoconjugates. Nat Commun **10:**1390. https://doi.org/10.1038/s41467-019-09362-z.
44. **Piesla MJ, Leventhal L, Strassle BW, Harrison JE, Cummons TA, Lu P, Whiteside GT.** 2009. Abnormal gait, due to inflammation but not nerve injury, reflects enhanced nociception in preclinical pain models. Brain Res **1295:**89–98. https://doi.org/10.1016/j.brainres.2009.07.091.
45. **Poropatich KO, Walker CL, Black RE.** 2010. Quantifying the association between *Campylobacter* infection and Guillain-Barre syndrome: a systematic review. J Health Popul Nutr **28:**545–552. https://doi.org/10.3329/jhpn.v28i6.6602.
46. **Prendergast MM, Moran AP.** 2000. Lipopolysaccharides in the development of the Guillain-Barre syndrome and Miller Fisher syndrome forms of acute inflammatory peripheral neuropathies. J Endotoxin Res **6:**341–359.
47. **Rathinam VA, Hoag KA, Mansfield LS**. 2008. Dendritic cells from C57BL/6 mice undergo activation and induce Th1-effector cell responses against *Campylobacter jejuni*. Microbes Infect **10**(12-13):1316-1324. https://doi.org/10.1016/j.micinf.2008.07.030.
48. **Rees JH, Gregson NA, Hughes RA.** 1995. Antiganglioside GM1 antibodies in Guillain-Barre syndrome and their relationship to *Campylobacter jejuni* infection. Ann Neurol **38:**809–816. https://doi.org/10.1002/ana.410380516.
49. **Reiner SL, Locksley RM.** 1995. The regulation of immunity to *Leishmania major*. Annu Rev Immunol **13:**151–177. https://doi.org/10.1146/annurev.iy.13.040195.001055.
50. **Sabat R, Grutz G, Warszawska K, Kirsch S, Witte E, Wolk K, Geginat J.** 2010. Biology of interleukin-10. Cytokine Growth Factor Rev **21:**331–344. https://doi.org/10.1016/j.cytogfr.2010.09.002.
51. **Salomon B, Rhee L, Bour-Jordan H, Hsin, H, Montag A, Soliven B, Arcella J, Girvin AM, Miller SD, Bluestone JA.** 2001. Development of spontaneous autoimmune peripheral polyneuropathy in B7-2-deficient NOD mice. J Exp Med **194:**677–684. https://doi.org/10.1084/jem.194.5.677.
52. **Schindelin J, Arganda-Carreras I, Frise E, Kaynig V, Longair M, Pietzch T, Preibisch S, Rueden C, Saalfeld S, Schmid B, Tinevez J-Y, White DJ, Hartenstein V, Eliceiri K, Tomancak P, Cardona A.** 2012. Fiji: an open-source platform for biological-image analysis. Nat Methods **9:**676–682. https://doi.org/10.1038/nmeth.2019.
53. **Schneider CA, Rasband WS, Eliceiri KW.** 2012. NIH Image to ImageJ: 25 years of image analysis. Nat Methods **9:**671–675. https://doi.org/10.1038/nmeth.2089.
54. **Sheikh KA, Nachamkin I, Ho TW, Willison HJ, Veitch H, Ung H, Nicholson M, Li CY, Wu HS, Shen BQ, Cornblath DR, Asbury AK, McKhann GM, Griffin JW.** 1998. *Campylobacter jejuni* lipopolysaccharides in Guillain-Barre syndrome. Neurology **51:**371–378. https://doi.org/10.1212/WNL.51.2.371.
55. **St Charles JL, Bell JA, Gadsden BJ, Malik A, Cooke H, Van de Grift LK, Kim HY, Smith EJ, Mansfield LS.** 2017. Guillain-Barre syndrome is induced in nonobese diabetic (NOD) mice following *Campylobacter jejuni* infection and is exacerbated by antibiotics. J Autoimmun **77:**11–38. https://doi.org/10.1016/j.jaut.2016.09.003.
56. **Stanciu GD, Solcan G.** 2016. Acute idiopathic polyradiculoneuritis concurrent with acquired myasthenia gravis in a West Highland white terrier dog. BMC Vet Res **12:**111. https://doi.org/10.1186/s12917-016-0729-1.
57. **van den Berg B, Walgaard C, Drenthen J, Fokke C, Jacobs BC, van Doorn PA.** 2014. Guillain-Barre syndrome: pathogenesis, diagnosis, treatment and prognosis. Nat Rev Neurol **10:**469–482. https://doi.org/10.1038/nrneurol.2014.121.
58. **Watanabe H, Numata K, Ito T, Takagi K, Matsukawa A.** 2004. Innate immune response in Th1- and Th2-dominant mouse strains. Shock **22:**460–466. https://doi.org/10.1097/01.shk.0000142249.08135.e9.
59. **Weaver CT, Harrington LE, Mangan PR, Gavrieli M, Murphy KM.** 2006. Th17: an effector CD4 T cell lineage with regulatory T cell ties. Immunity **24:**677–688. https://doi.org/10.1016/j.immuni.2006.06.002.
60. **World Health Organization.** [Internet]. 2017. Campylobacter fact sheet. [Cited 5 December 2021]. Available at http://www.who.int/mediacentre/factsheets/fs255/en/.
61. **Wilson DL, Abner SR, Newman TC, Mansfield LS, Linz JE.** 2000. Identification of ciprofloxacin-resistant Campylobacter jejuni by use of a fluorogenic PCR assay. J Clin Microbiol **38:**3971–3978. https://doi.org/10.1128/JCM.38.11.3971-3978.2000.
62. **Xia RH, Yosef N, Ubogu EE.** 2010. Clinical, electrophysiological and pathologic correlations in a severe murine experimental autoimmune neuritis model of Guillain-Barre syndrome. J Neuroimmunol **219:**54–63. https://doi.org/10.1016/j.jneuroim.2009.11.019.
63. **Yang F, Wang D, Li Y, Sang L, Zhu J, Wang J, Wei B, Lu C, Sun X.** 2017. Th1/Th2 balance and Th17/Treg-mediated immunity in relation to murine resistance to dextran sulfate-induced colitis. J Immunol Res **2017:**7047201. https://doi.org/10.1155/2017/7047201.
64. **Young KT, Davis LM, Dirita VJ.** 2007. *Campylobacter jejuni*: molecular biology and pathogenesis. Nat Rev Microbiol **5:**665–679. https://doi.org/10.1038/nrmicro1718.
65. **Yuki N, Susuki K, Koga M, Nishimoto Y, Odaka M, Hirata K, Taguchi K, Miyatake T, Furukawa K, Kobata T, Yamada M.** 2004. Carbohydrate mimicry between human ganglioside GM1 and *Campylobacter jejuni* lipooligosaccharide causes Guillain-Barre syndrome. Proc Natl Acad Sci USA **101:**11404–11409. https://doi.org/10.1073/pnas.0402391101.
66. **Yuki N, Taki T, Inagaki F, Kasama T, Takahashi M, Saito K, Handa S, Miyatake.** 1993. A bacterium lipopolysaccharide that elicits Guillain-Barre syndrome has a GM1 ganglioside-like structure. J Exp Med **178:**1771–1775. https://doi.org/10.1084/jem.178.5.1771.